

AD-A138 286

THE EFFECTS OF APERTURE ANTENNAS AFTER SIGNAL
PROPAGATION THROUGH ANISOTR. (U) MISSION RESEARCH CORP
SANTA BARBARA CA D L KNEPP 01 MAR 83 MRC-R-744
DNA-TR-81-254 DNA001-81-C-0006

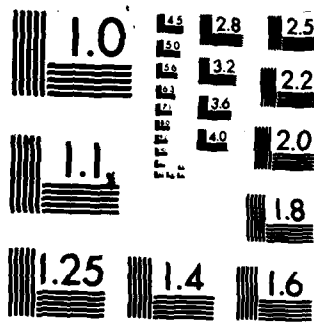
1/1

UNCLASSIFIED

F/G 20/14

NL

END
DATE
FORMED
36-84
DTIC



MICROCOPY RESOLUTION TEST CHART
NATIONAL BUREAU OF STANDARDS-1963-A

12

AD A138286

DNA-TR-81-254

THE EFFECTS OF APERTURE ANTENNAS
AFTER SIGNAL PROPAGATION THROUGH
ANISOTROPIC IONIZED MEDIA

Dennis L. Knepp
Mission Research Corporation
P.O. Drawer 719
Santa Barbara, California 93102

1 March 1983

Technical Report

CONTRACT No. DNA 001-81-C-0006

APPROVED FOR PUBLIC RELEASE;
DISTRIBUTION UNLIMITED.

DTIC
SELECTED
FEB 24 1984
A

THIS WORK WAS SPONSORED BY THE DEFENSE NUCLEAR AGENCY
UNDER RDT&E RMSS CODE B322082466 S99QAXHA00004 H2590D.

DTIC FILE COPY

Prepared for
Director
DEFENSE NUCLEAR AGENCY
Washington, DC 20305

84 01 20 024

Destroy this report when it is no longer
needed. Do not return to sender.

PLEASE NOTIFY THE DEFENSE NUCLEAR AGENCY,
ATTN: STTI, WASHINGTON, D.C. 20305, IF
YOUR ADDRESS IS INCORRECT, IF YOU WISH TO
BE DELETED FROM THE DISTRIBUTION LIST, OR
IF THE ADDRESSEE IS NO LONGER EMPLOYED BY
YOUR ORGANIZATION.



UNCLASSIFIED

SECURITY CLASSIFICATION OF THIS PAGE (When Data Entered)

REPORT DOCUMENTATION PAGE		READ INSTRUCTIONS BEFORE COMPLETING FORM
1 REPORT NUMBER DNA-TR-81-254	2 GOVT ACCESSION NO. ADA138 2X6	3 RECIPIENT'S CATALOG NUMBER
4 TITLE (and Subtitle) THE EFFECTS OF APERTURE ANTENNAS AFTER SIGNAL PROPAGATION THROUGH ANISOTROPIC IONIZED MEDIA		5 TYPE OF REPORT & PERIOD COVERED Technical Report
		6 PERFORMING ORG. REPORT NUMBER MRC-R-744
7 AUTHOR Dennis L. Knepp		8 CONTRACT OR GRANT NUMBER(s) DNA 001-81-C-0006
		10 PROGRAM ELEMENT, PROJECT, TASK AREA & WORK UNIT NUMBERS Task S99QAXHA-00004
9 PERFORMING ORGANIZATION NAME AND ADDRESS Mission Research Corporation P.O. Drawer 719 Santa Barbara, California 93102		12 REPORT DATE 1 March 1983
		13 NUMBER OF PAGES 74
11 CONTROLLING OFFICE NAME AND ADDRESS Director Defense Nuclear Agency Washington, D.C. 20305		15 SECURITY CLASS (of this report) UNCLASSIFIED
		15a DECLASSIFICATION DOWNGRADING SCHEDULE N/A since UNCLASSIFIED
14 MONITORING AGENCY NAME & ADDRESS (if different from Controlling Office)		
16 DISTRIBUTION STATEMENT (of this Report) Approved for public release; distribution unlimited.		
17 DISTRIBUTION STATEMENT (of the abstract entered in Block 20, if different from Report)		
18 SUPPLEMENTARY NOTES This work was sponsored by the Defense Nuclear Agency under RDT&E RMSS Code B322082466 S99QAXHA00004 H2590D.		
19 KEY WORDS (Continue on reverse side if necessary and identify by block number) Aperture Antennas Random Media Space Based Radar Dispersive Media Signal Scintillation Satellite Communications Ionospheric Propagation Frequency Selective Environment		
20 ABSTRACT (Continue on reverse side if necessary and identify by block number) Because of the large ranges involved, a space based search and track radar requires a large aperture antenna to increase the energy collected and to create a narrow beam for accurate angle measurements and for resistance to localized jammers. This report gives the effects of such an antenna on measurements of received power, decorrelation time (or distance), mean time delay, time delay jitter and coherence bandwidth after propagation of the radar signal through a strongly disturbed		

DD FORM 1473
1 JAN 73

EDITION OF 1 NOV 65 IS OBSOLETE

UNCLASSIFIED

SECURITY CLASSIFICATION OF THIS PAGE (When Data Entered)

UNCLASSIFIED

SECURITY CLASSIFICATION OF THIS PAGE(When Data Entered)

20. ABSTRACT (Continued)

transionospheric propagation channel. It is shown that aperture averaging can reduce observed signal power, increase observed decorrelation time and can be a significant factor in reducing the time delay jitter observed at the antenna output.

As part of this analysis an analytic solution is obtained for the two-position, two-frequency mutual coherence function for spherical wave propagation in the strong scatter limit. Transmitter and receiver are located in free-space on opposite sides of a thick slab containing anisotropic electron density irregularities that are elongated in the direction parallel to the magnetic field. The orientation of the magnetic field line with respect to the direction of propagation is arbitrary. This result is used to determine the effect of an antenna aperture as a function of geometry relative to the magnetic field.

UNCLASSIFIED

SECURITY CLASSIFICATION OF THIS PAGE(When Data Entered)

PREFACE

The author is indebted to Dr. Robert W. Stagat and Dr. Roger A. Dana of Mission Research Corporation and to Dr. Leon A. Wittwer of the Defense Nuclear Agency for their helpful discussions regarding this work.



6

Author	
Title	
Source	
Availability	
Distribution	
Availability	
Dist	Al

TABLE OF CONTENTS

<u>Section</u>		<u>Page</u>
	PREFACE	1
	LIST OF ILLUSTRATIONS	3
1	INTRODUCTION	5
2	FORMULATION	8
	2.1. MUTUAL COHERENCE FUNCTION	9
	2.2. IONIZATION IRREGULARITY DESCRIPTION	15
	2.2.1. Phase Standard Deviation	18
	2.3. ANALYTIC SOLUTION	19
	2.4. PHASE-SCREEN APPROXIMATION	29
	2.5. DECORRELATION DISTANCE	32
3	ANTENNA APERTURE EFFECTS ON RECEIVED SIGNAL	35
	3.1. APERTURE ANTENNA FORMULATION	36
	3.2. APERTURE DISTRIBUTION FUNCTION	46
	3.3. ANGULAR SCATTERING LOSS	47
	3.4. SIGNAL DECORRELATION DISTANCE	53
	3.5. ANTENNA APERTURE EFFECT ON $\langle \tau \rangle$ AND σ_{τ}	55
	3.5.1. Coherence Bandwidth	59
4	SUMMARY	62
	REFERENCES	63
APPENDIX	EVALUATION OF RMS ANGLE-OF-ARRIVAL FLUCTUATION	65

LIST OF ILLUSTRATIONS

<u>Figure</u>		<u>Page</u>
1.	Propagation of signals through a disturbed transionospheric channel.	8
2.	A single irregularity elongated along the magnetic field line in the y-z plane.	16
3.	Thin phase-screen propagation geometry.	33
4.	Receiving antenna aperture centered at origin of coordinate system.	38
5.	Angular scattering loss as a function of the magnetic field inclination angle.	52
6.	Angular scattering loss as a function of the aperture diameter.	52
7.	Effect of aperture and magnetic field direction on measured decorrelation distance in the x-direction.	54
8.	Effect of aperture and magnetic field direction on measured decorrelation distance in the x-direction.	54
9.	Effect of aperture and magnetic field direction on measurements of the decorrelation distance in the y-direction.	56
10.	Effect of aperture and magnetic field direction on measurements of the decorrelation distance in the y-direction.	56
11.	Effect of aperture and magnetic field direction on measurements of the coherence bandwidth.	60
12.	Effect of aperture and magnetic field direction on measurements of the coherence bandwidth.	60

SECTION 1 INTRODUCTION

Large high-gain antennas are used in many radar and communications applications to increase the energy collected, to increase angular accuracy, and to provide protection against jamming. If the wavefront at the antenna aperture experiences scintillation, large apertures can act to average the signal and thereby modify the observed signal properties. Aperture averaging is important for large lenses at optical wavelengths (Tatarskii, 1971) but is not generally important at satellite frequencies under ambient or naturally perturbed ionospheric conditions.

However, communications and radar systems from VHF to SHF that utilize trans-ionospheric propagation geometries can experience severe Rayleigh fading after a high altitude nuclear detonation. This increased level of scintillation is caused by the creation of great quantities of ionization which evolves into large irregular structure that takes the form of striations or filaments aligned along the earth's magnetic field. Since the velocity of propagation is dependent upon the local index-of-refraction, different portions of a wavefront propagate at different velocities in a striated region. Thus a once plane wavefront can become distorted with different portions traveling in slightly different directions. As the wave propagates farther, diffraction or angular scattering causes constructive and destructive interference which introduces fluctuations in amplitude, phase, and angle-of-arrival.

For cases of severe scintillation where the signal varies across the area of the receiving aperture, the effect of the aperture can be significant. It is well known that an aperture antenna acts to cut off energy that is incident at off-boresight angles where the antenna gain function is reduced. This effect may also be viewed as the result of averaging or coherent processing of the electromagnetic field received at the aperture location. In this report the effects of aperture averaging are analytically calculated for the situation where a Gaussian antenna beam is used by the receiver. It is shown that aperture averaging has a greater effect on antenna measurements of mean time delay and time delay jitter than on measurements of decorrelation time or scattering loss. Simple analytic expressions are given for all these quantities in terms of the geometry of the propagation path and the severity and structure of the ionization irregularities.

To obtain results applicable to a general geometry of the line-of-sight relative to the field aligned ionization structure, it is necessary to obtain an analytic solution for the two-position, two-frequency mutual coherence function for spherical wave propagation through a thick layer of anisotropic electron density irregularities. It is assumed here that strong scattering conditions prevail and that the quadratic approximation to the phase structure-function is valid.

This approximation was used by Sreenivasiah et al., (1976) and by Sreenivasiah and Ishimaru (1979) for the cases of plane wave and beam wave propagation in homogeneous turbulence. More recently the two-position, two-frequency mutual coherence function was obtained for spherical wave propagation using the extended Huygens-Fresnel principle (Fante, 1981). Although the quadratic structure-function approximation can sometimes lead to difficulties (Wandzura, 1980) it is appropriate for the two-frequency mutual coherence function but not for calculation of higher

moments of the field (Fante, 1980). Fante (1981) discusses the accuracy of the quadratic structure-function approximation for the case of atmospheric turbulence with a Kolmogorov power spectrum. He has found that the accuracy is a function of the irregularity power spectrum and of the strength of the turbulence (Private Communication, 1982), with accuracy increasing for stronger scattering.

This work is a generalization of an earlier calculation (Knepp, 1982) valid only for isotropic turbulence. As in the former study, the results here are specialized to the case of a thin phase-screen approximation to the thick scattering medium. With this simplification analytic results are obtained for the received impulse response function to a transmitted power delta function. Then results may easily be determined for the mean time delay and time delay jitter for strong, anisotropic turbulence in the thin phase-screen approximation. Results for these quantities in the thin phase-screen approximation have previously been shown (Knepp, 1982) to closely approximate the results for a thick scattering layer for the case of isotropic turbulence.

The effects of a Gaussian receiving antenna on measurements of received power, decorrelation time (or distance), mean time delay, time delay jitter and coherence bandwidth are determined. It is shown that aperture averaging can reduce observed signal power, increase observed decorrelation time and be a significant factor in reduced observed time-of-arrival jitter at the antenna output.

SECTION 2 FORMULATION

Consider a monochromatic spherical wave $E(\bar{\rho}, z, \omega, t)$ which originates from a transmitter located at $(0, 0, -z_t)$ and propagates in free-space in the positive z direction where it is incident on an ionization irregularity layer which extends from $0 \leq z \leq L$. After emerging from the layer at $z = L$, the wave then propagates in free-space to a receiver located at $(0, 0, z_r)$. This thick layer geometry is shown in Figure 1. As the wave propagates, its phase substantially behaves as $(-i\langle k \rangle z + i\omega t)$ so write

$$E(\bar{\rho}, z, \omega, t) = U(\bar{\rho}, z, \omega) \exp\{i(\omega t - \int \langle k(z') \rangle dz')\} \quad (1)$$

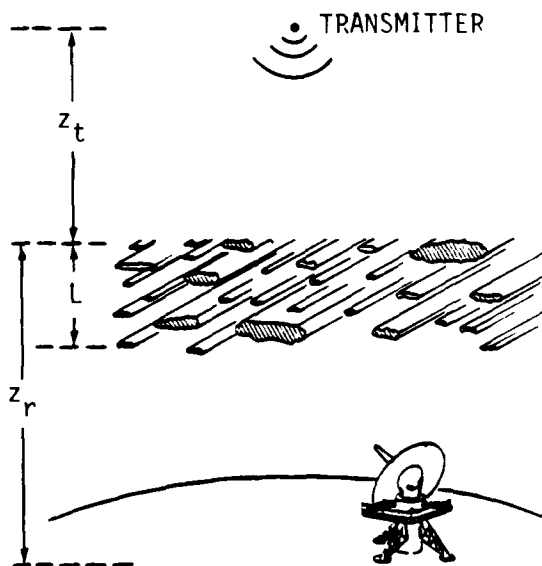


Figure 1. Propagation of signals through a disturbed transionospheric channel.

where $\langle k(z) \rangle$ is the mean wave number given by

$$\langle k(z) \rangle = \frac{\omega}{c} \left(1 - N_e/n_c\right)^{1/2} = k \left(1 - k_p^2/k^2\right)^{1/2} \quad (2)$$

where c is the speed of light in a vacuum, N_e is the mean ionization density, n_c is the critical electron density and is related to the classical electron radius r_e by $n_c = \pi/(\lambda^2 r_e)$, ($r_e = 2.82 \times 10^{-15}$ m).

It has been shown that $U(\bar{\rho}, z, \omega)$ satisfies the parabolic wave equation under the Markov approximation, (Tatarskii, 1971; Yeh and Liu, 1977)

$$\frac{\partial^2 U}{\partial z^2} - 2i\langle k(z) \rangle \frac{\partial U}{\partial z} - \langle k^2(z) \rangle \frac{\frac{\Delta N_e}{N_e} \frac{\omega_p^2}{\omega^2}}{(1 - \omega_p^2/\omega^2)} U = 0 \quad (3)$$

where ΔN_e is a small variation in the ionization level and $\omega_p = k_p c$ is the circular plasma frequency of the background ionization. The exponential time dependence has been suppressed and it has been assumed that $\omega_p \ll \omega$, otherwise signal attenuation would be the dominant effect.

2.1 MUTUAL COHERENCE FUNCTION

Now in the case that the transmitted waveform is no longer a monochromatic wave, but can be expressed as a waveform modulated on a carrier, the two-position, two-frequency mutual coherence function Γ is of interest. Γ is important for the calculation of pulse propagation in a random medium and it serves as a basis from which to calculate the important power impulse response function and its moments. Under the Markov approximation, Γ satisfies the following equation (Tatarskii, 1971; Yeh and Liu, 1977).

$$\frac{\partial \Gamma}{\partial z} + \frac{i}{2k_1 k_2} (k_2 \nabla_{\perp 1}^2 - k_1 \nabla_{\perp 2}^2) \Gamma - \frac{1}{8} [2k_1 \beta_1 k_2 \beta_2 A(\bar{\rho}_1 - \bar{\rho}_2) - (k_1^2 \beta_1^2 + k_2^2 \beta_2^2) A(0)] \Gamma = 0 \quad (4)$$

where

$$\Gamma = \langle U(x_1, y_1, z, \omega_1) U^*(x_2, y_2, z, \omega_2) \rangle$$

and k_1 and k_2 are the wavenumbers at two frequencies ω_1 and ω_2 , respectively, and $\nabla_{\perp 1}^2$ is the two-dimensional Laplacian

$$\nabla_{\perp 1}^2 = \frac{\partial^2}{\partial x_1^2} + \frac{\partial^2}{\partial y_1^2}$$

with a similar definition for $\nabla_{\perp 2}^2$. Following Yeh and Liu (1977) let

$$\beta_1 = \frac{\omega_p^2 / \omega_1^2}{1 - \omega_p^2 / \omega_1^2} \quad (5)$$

with a similar definition for β_2 .

The function $A(\bar{\rho})$ is the integral of the autocorrelation function of electron density fluctuations, B_{ξ} , in the direction of propagation

$$A(\bar{\rho}_1 - \bar{\rho}_2) = \int_{-\infty}^{\infty} B_{\xi}(\bar{\rho}_1 - \bar{\rho}_2, z') dz' \quad (6)$$

where

$$\bar{\rho}_1 - \bar{\rho}_2 = (x_1 - x_2, y_1 - y_2)$$

$$\xi = \frac{\Delta N_e}{\langle N_e \rangle}$$

so that

$$A(\bar{\rho}_1 - \bar{\rho}_2) = 2\pi \int_{-\infty}^{\infty} \int_{-\infty}^{\infty} e^{i\bar{K}_{\perp} \cdot (\bar{\rho}_1 - \bar{\rho}_2)} \phi_{\xi}(\bar{K}_{\perp}, K_z=0) d^2 K_{\perp} \quad (7)$$

where ϕ_{ξ} is the power spectrum of electron density fluctuations. Equations 6 and 7 depend upon the validity of the Markov approximation where it is assumed that the electron density fluctuations are delta-correlated in the direction of propagation (Fante, 1975). That is

$$\beta_{\xi}(\bar{\rho}_1 - \bar{\rho}_2, z_1 - z_2) = A(\bar{\rho}_1 - \bar{\rho}_2) \delta(z_1 - z_2) \quad (8)$$

Now the sum and difference substitutions

$$X = (x_1 + x_2)/2$$

$$\zeta = x_1 - x_2$$

$$Y = (y_1 + y_2)/2$$

$$\eta = y_1 - y_2$$

$$k_s = (k_1 + k_2)/2$$

$$k_d = k_1 - k_2$$

and the assumption that the frequencies of interest are much greater than the plasma frequency so that

$$\beta_1 = \omega_p^2 / \omega_1^2$$

$$\beta_2 = \omega_p^2 / \omega_2^2$$

enable Equation 4 to be rewritten as

$$\begin{aligned} \frac{\partial \Gamma}{\partial z} - \frac{i}{2(k_s^2 - k_d^2/4)} [k_d \nabla_d^2 + \frac{1}{4} k_d \nabla_s^2 - 2k_s \nabla_s \cdot \nabla_d] \Gamma \\ - \frac{1}{8} \left[\frac{2k_p^4}{k_1 k_2} A(\zeta, \eta) - \left(\frac{1}{k_1^2} + \frac{1}{k_2^2} \right) k_p^4 A(0) \right] \Gamma = 0 \end{aligned} \quad (9)$$

where

$$\nabla_d^2 = \frac{\partial^2}{\partial \zeta^2} + \frac{\partial^2}{\partial \eta^2}$$

$$\nabla_s^2 = \frac{\partial^2}{\partial \chi^2} + \frac{\partial^2}{\partial \gamma^2}$$

$$\nabla_s \cdot \nabla_d = \frac{\partial^2}{\partial \zeta \partial \chi} + \frac{\partial^2}{\partial \eta \partial \gamma}$$

Γ is now written in terms of the above sum and difference arguments as $\Gamma(\zeta, \eta, z, \omega)$ where $\omega = ck_d$.

The unknown two-frequency mutual coherence function may be written as $\Gamma = \Gamma_1 \Gamma_0$ where Γ_0 is the exact free-space solution in the parabolic approximation

$$\Gamma_0 = \left(\frac{1}{z+z_t} \right)^2 \exp \left\{ \frac{-ik_1(x_1^2+y_1^2) + ik_2(x_2^2+y_2^2)}{2(z+z_t)} \right\} \quad (10)$$

which under the sum and difference transformation used previously becomes

$$\Gamma_0 = \left(\frac{1}{z+z_t} \right)^2 \exp \left\{ \frac{-ik_s(\zeta X + \eta Y) - ik_d[(X^2+Y^2)/2 + (\zeta^2+\eta^2)/8]}{(z+z_t)} \right\} \quad (11)$$

Substituting $\Gamma = \Gamma_1 \Gamma_0$ into Equation 9 and neglecting near zone terms of the order of $k_s \zeta^2 / (z+z_t)$ and smaller, one obtains

$$\begin{aligned} \frac{\partial \Gamma_1}{\partial z} - \frac{1}{2} \frac{k_d}{(k_s^2 - k_d^2/4)} \nabla_d^2 \Gamma_1 + \frac{1}{(z+z_t)} \left[\zeta \frac{\partial}{\partial \zeta} + \eta \frac{\partial}{\partial \eta} \right] \Gamma_1 \\ - \frac{1}{8} \left[\frac{2k_p^4 A(\zeta, \eta)}{k_1 k_2} - \left(\frac{1}{k_1^2} + \frac{1}{k_2^2} \right) k_p^4 A(0) \right] \Gamma_1 \\ + \text{terms with } \frac{\partial \Gamma_1}{\partial X} + \frac{\partial \Gamma_1}{\partial Y} = 0 \end{aligned} \quad (12)$$

Equation 12 is valid in the region $0 \leq z \leq L$ with boundary condition

$$\Gamma_1(\zeta, \eta, z=0, \omega_d) = 1 \quad (13)$$

Since the boundary condition is independent of X and Y, and the equation has no terms other than the derivatives with respect to X and Y, it is apparent that

$$\frac{\partial \Gamma_1}{\partial X} = \frac{\partial \Gamma_1}{\partial Y} = 0$$

Now the substitutions

$$z' = z + z_t \quad (14a)$$

$$\theta = \zeta/z' = \zeta/(z+z_t) \quad (14b)$$

$$\phi = \eta/z' = \eta/(z+z_t) \quad (14c)$$

yield the following

$$\begin{aligned} \frac{\partial \Gamma_1}{\partial z'} - \frac{i}{2} \frac{k_d}{(k_s^2 - k_d^2/4)} \frac{1}{z'^2} \left[\frac{\partial^2}{\partial \theta^2} + \frac{\partial^2}{\partial \phi^2} \right] \Gamma_1 \\ - \frac{1}{8} \left[\frac{2k_p^4 A(z'(\theta+\phi))}{k_1 k_2} - \left(\frac{1}{k_2^2} + \frac{1}{k_1^2} \right) k_p^4 A(0) \right] \Gamma_1 = 0 \end{aligned} \quad (15)$$

The additional substitution $\Gamma_1 = \Gamma_2 \Gamma_3$ where

$$\Gamma_3 = \exp \left\{ - \frac{1}{8} A(0) (z' - z_t) k_p^4 \left(\frac{1}{k_1} - \frac{1}{k_2} \right)^2 \right\} \quad (16)$$

yields the simplified equation for Γ_2

$$\frac{\partial \Gamma_2}{\partial z'} - \frac{i k_d}{2 k_s^2} \frac{1}{z'^2} \left[\frac{\partial^2}{\partial \theta^2} + \frac{\partial^2}{\partial \phi^2} \right] \Gamma_2 - \frac{1}{4} \frac{k_p^4}{k_s^2} [A(z', \theta, z', \phi) - A(0)] \Gamma_2 = 0 \quad (17)$$

where k_d has been neglected with respect to k_s . The effect of this assumption is to restrict the validity of the solution to a small range of wavelengths centered about k_s . In the following k_s , the average wavenumber, will be replaced by k_0 , the wavenumber at the carrier frequency.

Equation 17 can only be solved analytically for the case where the function $A(z', \theta, z', \phi)$ can be represented as a quadratic. This is the well known quadratic phase structure-function approximation (Sreenivasiah et al. (1976); Sreenivasiah and Ishimaru (1979)). At this point it is necessary to determine the form of A for the irregularity spectrum of interest here.

2.2 IONIZATION IRREGULARITY DESCRIPTION

Here the ionization irregularities are assumed to be elongated along the direction of the earth's magnetic field. Figure 2 shows the geometry of the irregularities. The electromagnetic wave propagates in the negative z direction. The magnetic field vector lies in the y - z plane at an angle of ψ with respect to the z axis. The ionization irregularities are assumed rotationally symmetric with autocorrelation function

$$B_{\xi}(r, s) = \frac{\sigma_{N_e}^2}{\langle N_e \rangle^2} \exp \left\{ - \frac{r^2}{r_0^2} - \frac{s^2}{(qr_0)^2} \right\} \quad (18)$$

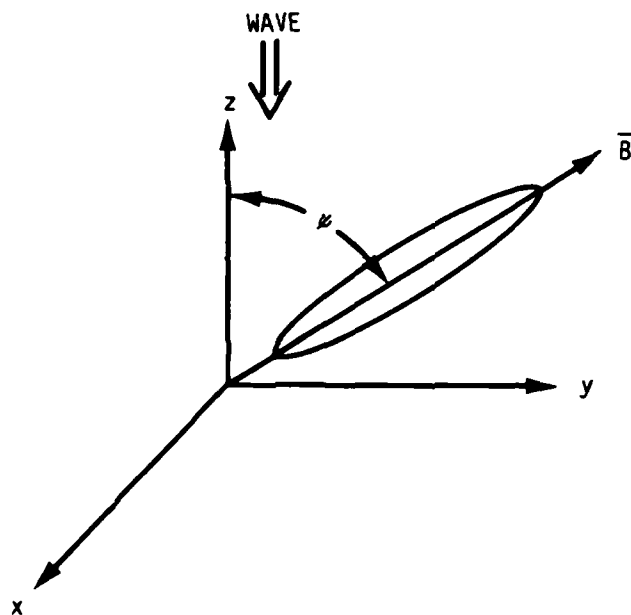


Figure 2. A single irregularity elongated along the magnetic field line in the y-z plane.

where s is measured along the magnetic field direction and r is measured perpendicular to the magnetic field direction. The quantity q is known as the axial ratio (Briggs and Parkin, 1963) and r_0 is the correlation distance or irregularity scale size.

The s, r coordinate system may be related to the x, y, z system by the equations

$$s^2 = (y \sin \psi + z \cos \psi)^2 \quad (19)$$

$$r^2 = x^2 + (y \cos \psi - z \sin \psi)^2 \quad (20)$$

Using the above transformation the irregularity correlation function may be expressed in the x, y, z system as

$$B_{\xi}(x,y,z) = \frac{\sigma_{N_e}^2}{\langle N_e \rangle^2} \exp \left\{ -\frac{x^2}{r_0^2} - \frac{y^2}{q^2 r_0^2} (q^2 \cos^2 \psi + \sin^2 \psi) \right. \\ \left. + \frac{2yz \sin \psi \cos \psi}{q^2 r_0^2} (q^2 - 1) - \frac{z^2}{q^2 r_0^2} (q^2 \sin^2 \psi + \cos^2 \psi) \right\} \quad (21)$$

The function $A(\zeta, \eta)$ as given by Equation 6 may then be easily obtained as

$$A(\zeta, \eta) = \frac{\sigma_{N_e}^2 \sqrt{\pi} q r_0}{\langle N_e \rangle^2 (q^2 \sin^2 \psi + \cos^2 \psi)^{1/2}} \\ \times \exp \left\{ -\frac{\zeta^2}{r_0^2} - \frac{\eta^2}{r_0^2 (q^2 \sin^2 \psi + \cos^2 \psi)} \right\} \quad (22)$$

The above equation is essentially Equation 10 in Briggs and Parkin (1963). $A(\zeta, \eta)$ is easily expanded in a Taylor series and, retaining only terms up to the quadratic, one obtains

$$A(\zeta, \eta) \approx A_0 + A_2 \zeta^2 + \Delta^2 A_2 \eta^2 \quad (23)$$

where

$$A_0 = \frac{\sigma_{N_e}^2 \sqrt{\pi} q r_0 \Delta}{\langle N_e \rangle^2} \quad (24)$$

$$A_2 = \frac{-\sigma_{N_e}^2 \sqrt{\pi} q \Delta}{\langle N_e \rangle^2 r_0} \quad (25)$$

$$\Delta^2 = \frac{1}{q^2 \sin^2 \psi + \cos^2 \psi} \quad (26)$$

This same formalism may also be applied to irregularity power spectra that are non-Gaussian. For the case of a power-law PSD the coefficients A_0 and A_2 are different than above but behave in essentially the same manner as a function of the outer scale size as long as the three-dimensional in-situ electron density PSD falls off at least as rapidly as K^{-4} .

2.2.1 Phase Standard Deviation

It is useful to establish the relationship between the coefficient A_0 and the variance of phase fluctuations σ_ϕ^2 . For a layer of thickness L greater than the correlation length of the irregularities the autocorrelation function of the phase is (Salpeter, 1967)

$$\langle \Delta\phi(x_1, y_1) \Delta\phi(x_2, y_2) \rangle = \frac{L k_0^2 \langle N_e \rangle^2}{4n_c^2} \int_{-\infty}^{\infty} B_\xi(\bar{\rho}_1 - \bar{\rho}_2, \eta) d\eta \quad (27)$$

Evaluation of this expression at $\bar{\rho}_1 - \bar{\rho}_2 = 0$ yields

$$\sigma_\phi^2 = \frac{k_0^2 \langle N_e \rangle^2}{4n_c^2} L A_0 = \frac{1}{4} k_p^4 L A_0 / k_0^2 \quad (28)$$

where Equation 6 is used for A_0 .

For the anisotropic correlation function given by Equation 18, the quantity A_0 or $A(0)$ is given by Equation 24 and

$$\sigma_\phi^2 = \sqrt{\pi} (\lambda r_e)^2 q \Delta r_0 L \sigma_{N_e}^2 \quad (29)$$

where the relationships $n_c = \pi/(\lambda^2 r_e)$ and $k_0 = 2\pi/\lambda$ have been used in Equation 28.

2.3 ANALYTIC SOLUTION

Now that expressions for A_0 , A_2 and σ_ϕ^2 have been obtained it is possible to proceed to an analytic solution for Γ . Recognizing that $A(0)$ and A_0 are identical, the quadratic structure-function approximation may be used in Equation 17 to eliminate $A(0)$. With the additional substitutions

$$a = \frac{1}{2} k_d/k_0^2 \quad (30a)$$

$$b = \frac{1}{4} k_p^4/k_0^2 \quad (30b)$$

$$v = (abA_2)^{1/2} z' = a_1 z' \quad (31a)$$

$$\mu = \left(\frac{1}{a^3 b A_2} \right)^{1/4} \theta = a_2 \theta \quad (31b)$$

$$\epsilon = \left(\frac{1}{a^3 b A_2} \right)^{1/4} \phi = a_2 \phi \quad (31c)$$

and the quadratic phase structure-function approximation given by Equation 23, Equation 17 may be written as

$$\frac{\partial \Gamma_2}{\partial v} - i \frac{1}{v^2} \left[\frac{\partial^2}{\partial \mu^2} + \frac{\partial^2}{\partial \epsilon^2} \right] \Gamma_2 - (\mu^2 + \Delta^2 \epsilon^2) v^2 \Gamma_2 = 0 \quad (32)$$

With these substitutions, the boundary condition describing the mutual coherence function at the transmitter is

$$\Gamma_2(\mu, \epsilon, v=a_1 z_t, \omega_d) = 1 \quad (33)$$

An analytic solution of the form

$$\Gamma_2 = f(v) \exp\{-g(v)\mu^2 - h(v)\epsilon^2\} \quad (34)$$

may be substituted into Equation 32 to obtain the following three equations

$$g' + \frac{i4g^2}{v^2} + v^2 = 0 \quad (35)$$

$$h' + \frac{i4h^2}{v^2} + \Delta^2 v^2 = 0 \quad (36)$$

$$f' + \frac{i2f(g+h)}{v^2} = 0 \quad (37)$$

Equation 35 represents the coefficients of terms from Equation 32 that are factors of μ^2 ; Equation 36 consists of the terms that are factors of ϵ^2 ; Equation 37 consists of terms that are independent of μ and ϵ .

Additional simplification results from the substitutions

$$g = v^2 G \quad (38)$$

$$h = v^2 H \quad (39)$$

which enable the three equations to be written as

$$G' v^2 + 2vG + i4v^2 G^2 = -v^2 \quad (40)$$

$$H' v^2 + 2vH + i4v^2 H^2 = -\Delta^2 v^2 \quad (41)$$

$$f' + i2f(G+H) = 0 \quad (42)$$

It is not difficult to solve Equations 40 and 41. The results may be written as

$$G(v) = \frac{i}{4v} - \frac{1}{\beta} \tanh(\beta v + C_1) \quad (43)$$

$$H(v) = \frac{i}{4v} - \frac{\Delta}{\beta} \tanh(\Delta \beta v + C_2) \quad (44)$$

where

$$\beta^2 = -i4 \quad (45)$$

and C_1 and C_2 are constants yet to be determined. With G and H known, f can be determined by direct integration of Equation 42 with the result

$$f(v) = v [\cosh(\beta v + C_1) \cosh(\Delta \beta v + C_2)]^{-1/2} C_3 \quad (46)$$

where C_3 is another constant yet to be determined.

Equations 38-39 and 43-45 may be combined to yield the result for Γ_2

$$\Gamma_2 = C_3 v [\cosh(\beta v + C_1) \cosh(\Delta \beta v + C_2)]^{-1/2} \times \exp \left\{ -\frac{iv}{4} (\mu^2 + \epsilon^2) + \frac{v^2}{\beta} [\mu^2 \tanh(\beta v + C_1) + \Delta \epsilon^2 \tanh(\Delta \beta v + C_2)] \right\} \quad (47)$$

The boundary condition given by Equation 33 is met by requiring that the coefficients of μ and ϵ are zero at $v = v_t$ and by requiring that Γ_2 be unity at $v = v_t$ for zero μ and ϵ . Mathematically

$$\frac{-i v_t}{4} + \frac{v_t^2}{\beta} \tanh(\beta v_t + C_1) = 0 \quad (48)$$

$$\frac{-i v_t}{4} + \frac{\Delta v_t^2}{\beta} \tanh(\Delta \beta v_t + C_2) = 0 \quad (49)$$

$$C_3 v_t [\cosh(\beta v_t + C_1) \cosh(\Delta \beta v_t + C_2)]^{-1/2} = 1 \quad (50)$$

The solutions to Equations 48 and 49 may be found as

$$\begin{aligned} C_1 &= -\beta v_t + \ln \left(\frac{\beta + 1/v_t}{\beta - 1/v_t} \right)^{1/2} \\ &= -\beta v_t + C_1' \end{aligned} \quad (51)$$

$$\begin{aligned} C_2 &= -\Delta \beta v_t + \ln \left(\frac{\Delta \beta + 1/v_t}{\Delta \beta - 1/v_t} \right)^{1/2} \\ &= -\Delta \beta v_t + C_2' \end{aligned} \quad (52)$$

where the new constants C_1' and C_2' are introduced for later convenience. Equations 51 and 52 may now be used in 50 to obtain the constant C_3 as

$$C_3 = \frac{1}{v_t} [\cosh C_1' \cosh C_2']^{1/2} \quad (53)$$

The expressions for the constants C_1 , C_2 and C_3 may now be inserted into the solution for Γ_2 with the result

$$\Gamma_2 = \frac{v}{v_t} \left\{ \frac{\cosh C_1' \cosh C_2'}{\cosh [\beta(v-v_t)+C_1'] \cosh [\Delta\beta(v-v_t)+C_2']} \right\}^{1/2} \quad (54)$$

$$\times \exp \left\{ -\frac{iv}{4} (\mu^2 + \epsilon^2) + \frac{v^2}{\beta} [\mu^2 \tanh[\beta(v-v_t)+C_1'] + \Delta\epsilon^2 \tanh[\Delta\beta(v-v_t)+C_2']] \right\}$$

This result is valid for propagation within the random slab from $z=0$ to $z=L$ or equivalently from $v=v_t$ to $v=v_t+v_L$.

In keeping with the approximation $k_d \ll k_0$, Γ_2 from Equation 16 may be written as

$$\Gamma_3 \approx \exp \left\{ -\frac{A_0 (z'-z_t) k_p^4 k_d^2}{8k_0^4} \right\} \quad (55)$$

At the far edge of the thick scattering layer, $z=L$ or $z'=z_t+L$ and Γ_3 becomes

$$\Gamma_3 \approx \exp \left\{ -\frac{A_0 L k_p^4 k_d^2}{8k_0^4} \right\} \quad (56)$$

which may be written as

$$\Gamma_3 \approx \exp \left\{ -\frac{\sigma_\phi^2 \omega_d^2}{2\omega_0^2} \right\} \quad (57)$$

where σ_ϕ^2 is obtained from Equation 28.

At this point Equations 54 and 57 may be multiplied to give the value of Γ_1 at the exit of the thick scattering layer:

$$\begin{aligned} \Gamma_1(\theta, \phi, z'=L+z_t, \omega_d) &= \exp\left\{-\frac{\sigma_\phi^2 \omega_d^2}{2\omega_0^2}\right\} \\ &\times \left(\frac{L+z_t}{z_t}\right) \left\{\frac{\cosh C_1' \cosh C_2'}{\cosh(\beta a_1 L + C_1') \cosh(\Delta\beta a_1 L + C_2')}\right\}^{1/2} \\ &\times \exp\left\{-\frac{i(L+z_t)a_1 a_2^2}{4}(\theta^2 + \phi^2)\right. \\ &\left. + \frac{(L+z_t)^2 a_1^2 a_2^2}{\beta} [\theta^2 \tanh(\beta a_1 L + C_1') + \Delta\phi^2 \tanh(\Delta\beta a_1 L + C_2')]\right\} \quad (58) \end{aligned}$$

For temporary algebraic convenience let this be written as

$$\begin{aligned} \Gamma_1(\theta, \phi, z'=L+z_t, \omega_d) &= \\ &F \exp\{-(A-Bt)\theta^2 - (A-\Delta Bt')\phi^2\} \quad (59) \end{aligned}$$

where

$$\begin{aligned} F &= \exp\left\{-\frac{\sigma_\phi^2 \omega_d^2}{2\omega_0^2}\right\} \\ &\times \left(\frac{L+z_t}{z_t}\right) \left\{\frac{\cosh C_1' \cosh C_2'}{\cosh(\beta a_1 L + C_1') \cosh(\Delta\beta a_1 L + C_2')}\right\} \quad (60) \end{aligned}$$

$$A = \frac{i(L+z_t) a_1 a_2^2}{4} \quad (61)$$

$$B = \frac{(L+z_t)^2 a_1^2 a_2^2}{\beta} \quad (62)$$

$$t = \tanh (\beta a_1 L + C_1') \quad (63)$$

$$t' = \tanh (\Delta \beta a_1 L + C_2') \quad (64)$$

Although the above expressions are sufficient, considerable simplification occurs later, in the thin phase-screen approximation, if all the hyperbolic functions of sums in Equations 60, 63 and 64 are expanded. The expansions require the functions $\tanh C_1'$ and $\tanh C_2'$. These two quantities are easily calculated as

$$\begin{aligned} \tanh C_1' &= \tanh \left[\ln \left(\frac{\beta + 1/v_t}{\beta - 1/v_t} \right)^{1/2} \right] \\ &= \frac{1}{\beta v_t} = \frac{1}{\beta a_1 z_t} \end{aligned} \quad (65)$$

$$\begin{aligned} \tanh C_2' &= \tanh \left[\ln \left(\frac{\Delta \beta + 1/v_t}{\Delta \beta - 1/v_t} \right)^{1/2} \right] \\ &= \frac{1}{\Delta \beta v_t} = \frac{1}{\Delta \beta a_1 z_t} \end{aligned} \quad (66)$$

The function F can then be written as

$$F = \exp \left\{ - \frac{\sigma_{\phi}^2 \omega_d^2}{2\omega_0^2} \right\} \beta a_1 (L+z_t) \times \left\{ \frac{\Delta}{(\beta a_1 z_t \cosh \beta a_1 L + \sinh \beta a_1 L)(\Delta \beta a_1 z_t \cosh \Delta \beta a_1 L + \sinh \Delta \beta a_1 L)} \right\}^{1/2} \quad (67)$$

Similarly

$$t = \frac{1 + \beta a_1 z_t \tanh \beta a_1 L}{\beta a_1 z_t + \tanh \beta a_1 L} \quad (68)$$

$$t' = \frac{1 + \Delta \beta a_1 z_t \tanh \Delta \beta a_1 L}{\Delta \beta a_1 z_t + \tanh \Delta \beta a_1 L} \quad (69)$$

To complete the solution it is necessary to solve for Γ_1 in the region $z \geq L$ or $z' \geq L+z_t$. Equation 58 serves as the boundary condition at $z' = L+z_t$. Since the region $z' \geq L+z_t$ corresponds to free-space with no ionization, Equation 15 is appropriate where the last term, which is dependent on the function A, may be neglected since A is zero in the absence of ionization irregularities. Also, in keeping with previous assumptions, the k_d^2 term is ignored with respect to the k_s^2 term in Equation 15.

The Fourier transform pair

$$\Gamma_1(\theta, \phi, z', \omega_d) = \int_{-\infty}^{\infty} \int_{-\infty}^{\infty} e^{i(K_{\theta}\theta + K_{\phi}\phi)} \hat{\Gamma}_1(K_{\theta}, K_{\phi}, z', \omega_d) dK_{\theta} dK_{\phi} \quad (70)$$

$$\hat{\Gamma}_1(K_{\theta}, K_{\phi}, z', \omega_d) = (1/2\pi)^2 \int_{-\infty}^{\infty} \int_{-\infty}^{\infty} e^{-i(K_{\theta}\theta + K_{\phi}\phi)} \Gamma_1(\theta, \phi, z', \omega_d) d\theta d\phi \quad (71)$$

may be substituted into the suitably modified Equation 15 to obtain the algebraic equation

$$\frac{\partial \hat{\Gamma}_1}{\partial z'} + \frac{i k_d}{2 k_0^2} \frac{1}{z'^2} (K_\theta^2 + K_\phi^2) \hat{\Gamma}_1 = 0 \quad (72)$$

where k_s has been replaced by k_0 , the wavenumber at the carrier frequency.

Equation 72 may be solved and the boundary condition 59 applied at $z' = L + z_t$ with the result

$$\begin{aligned} \hat{\Gamma}_1(K_\theta, K_\phi, z_t + z_r, \omega_d) &= \hat{\Gamma}_1(K_\theta, K_\phi, L + z_t, \omega_d) \\ &\times \exp[-i\gamma(K_\theta^2 + K_\phi^2)] \end{aligned} \quad (73)$$

where

$$\gamma = \frac{1}{2} \frac{k_d}{k_s^2} \frac{(z_r - L)}{(L + z_t)(z_t + z_r)} \quad (74)$$

The final result may then be obtained by taking the Fourier transform of Equation 59 to obtain $\hat{\Gamma}_1(K_\theta, K_\phi, z' + z_t, \omega_d)$ and then taking the inverse Fourier transform of Equation 73. The appropriate Fourier transform pair is given by Equations 70 and 71.

The Fourier transform of Equation 59 is easily obtained as

$$\begin{aligned} \hat{\Gamma}_1(K_\theta, K_\phi, z' = L + z_t, \omega_d) &= \frac{F}{4\pi} \\ &\times \frac{1}{(A - Bt)^{1/2} (A - \Delta Bt')^{1/2}} \\ &\times \exp \left\{ -\frac{K_\theta^2}{4(A - Bt)} - \frac{K_\phi^2}{4(A - \Delta Bt')} \right\} \end{aligned} \quad (75)$$

According to Equation 73 this expression is multiplied by the appropriate factor to account for free-space propagation and the inverse transform taken to obtain as the final result

$$\Gamma_1(\theta, \phi, z' = z_t + z_r, \omega_d) = \frac{F}{[(1+i4\gamma(A-Bt)) (1+i4\gamma(A-\Delta Bt'))]^{1/2}} \times \exp \left\{ -\frac{\theta^2(A-Bt)}{1+i4\gamma(A-Bt)} - \frac{\phi^2(A-\Delta Bt')}{1+i4\gamma(A-\Delta Bt')} \right\} \quad (76)$$

Utilizing the relationships given by Equations 14b-c at the receiver location,

$$\theta = \zeta / (z_t + z_r)$$

$$\phi = n / (z_t + z_r)$$

Equation 76 may be written in final form as

$$\Gamma_1(\zeta, n, z_t + z_r, \omega_d) = \frac{F}{[(1+i4\gamma(A-Bt)) (1+i4\gamma(A-\Delta Bt'))]^{1/2}} \times \exp \left\{ -\frac{\zeta^2(A-Bt)/(z_t + z_r)^2}{1+i4\gamma(A-Bt)} - \frac{n^2(A-\Delta Bt')/(z_t + z_r)^2}{1+i4\gamma(A-\Delta Bt')} \right\} \quad (77)$$

Equation 77 is the result for Γ_1 after propagation through a thick layer. The full solution for the two-position, two-frequency mutual coherence function is obtained by multiplication by Γ_0 as given by Equation 11. Γ_0 is not affected by the random layer and may be ignored in the following.

2.4 PHASE-SCREEN APPROXIMATION

Much simplification is possible if the thick scattering layer is replaced by an equivalent thin phase-screen of infinitesimal thickness and the same overall phase variance. To the first order, in the thin phase-screen approximation

$$\cosh \Delta\alpha a_1 L \approx 1 \quad (78a)$$

$$\sinh \Delta\alpha a_1 L \approx \Delta\alpha a_1 L \quad (78b)$$

$$\tanh \Delta\alpha a_1 L \approx \Delta\alpha a_1 L \quad (78c)$$

With the above approximations it is easy to show that

$$F \approx \exp \left\{ - \frac{\sigma_\phi^2 \omega_d^2}{2\omega_0^2} \right\} \quad (79)$$

Similarly, the coefficient of ϕ^2 can be written as

$$\begin{aligned} A - \Delta B t' &\approx \frac{1(L+z_t) a_1 a_2^2}{4} \\ &- \frac{\Delta(L+z_t)^2 a_1^2 a_2^2}{\beta} \left(\frac{1 + \Delta^2 \beta^2 a_1^2 z_t^2 L}{\Delta \beta a_1 (L+z_t)} \right) \\ &= -\Delta^2 a_1^2 a_2^2 L z_t^2 \end{aligned} \quad (80)$$

where $\beta^2 = -i4$ is used to simplify the result. The quantities a_1 and a_2 are given by Equations 30 and 31 and may be substituted into Equation 80 to obtain

$$\begin{aligned} A - \Delta B t' &\approx - \Delta^2 b A_2 L z_t^2 \\ &= - \frac{\Delta^2 k^4 A_2 L z_t^2}{4k_0^2} \end{aligned} \quad (81)$$

This equation may be simplified by substituting the expression for σ_ϕ^2 given by Equation 28 to yield

$$A - \Delta B t' \approx - \frac{\Delta^2 \sigma_\phi^2 A_2 z_t^2}{A_0} \quad (82)$$

Similarly

$$A - B t \approx - \frac{\sigma_\phi^2 A_2 z_t^2}{A_0} \quad (83)$$

The final quantity of interest in this phase-screen approximation is

$$\begin{aligned} 4\gamma(A - \Delta B t') &\approx - \frac{2\Delta^2 k_d^2 z_r z_t \sigma_\phi^2 A_2}{k_0^2 (z_t + z_r) A_0} \\ &= - \frac{\Delta^2 \omega_d \lambda z_r z_t \sigma_\phi^2 A_2}{\pi \omega_0 (z_t + z_r) A_0} \end{aligned} \quad (84)$$

Similarly

$$4\gamma(A - B t) \approx - \frac{\omega_d \lambda z_r z_t \sigma_\phi^2 A_2}{\pi \omega_0 (z_t + z_r) A_0} \quad (85)$$

Now in this phase-screen approximation the result for the two-position, two-frequency mutual coherence function may be written as

$$\Gamma_1(\xi, \eta, z_t + z_r, \omega_d) = \left\{ \frac{1}{\left(1 + i \frac{\omega_d}{\omega'}\right) \left(1 + i \frac{\omega_d}{\omega' / \Delta^2}\right)} \right\}^{1/2} \times \exp \left\{ - \frac{\sigma_\phi^2 \omega_d^2}{2\omega_0^2} \right\} \exp \left\{ - \frac{\zeta^2 / \lambda_0^2}{\left(1 + i \frac{\omega_d}{\omega'}\right)} - \frac{\eta^2 / (\lambda_0^2 / \Delta^2)}{\left(1 + i \frac{\omega_d}{\omega' / \Delta^2}\right)} \right\} \quad (86)$$

where

$$\lambda_0^2 = - \frac{(z_t + z_r)^2 A_0}{z_t^2 \sigma_\phi^2 A_2} \quad (87)$$

$$\omega' = - \frac{\pi \omega_0 (z_t + z_r) A_0}{\lambda z_r z_t \sigma_\phi^2 A_2} \quad (88)$$

Equations 86-88 are valid for any anisotropic power spectrum for which, in the strong scattering limit, the phase structure-function can be expanded in the form of Equation 23. For the anisotropic Gaussian power spectrum of interest in this work

$$\frac{A_0}{A_2} = - r_0^2 \quad (89)$$

The phase variance is given by Equation 29 so that for the Gaussian PSD

$$\lambda_0^2 = \frac{(z_t + z_r)^2 r_0}{\sqrt{\pi} (\lambda r_e)^2 q \Delta L z_t^2 \sigma_{N_e}^2} \quad (90)$$

$$\omega' = \frac{2\pi^{3/2} c (z_t + z_r) r_0}{r_e^2 \lambda^4 z_r z_t q \Delta L \sigma_{N_e}^2} \quad (91)$$

2.5 DECORRELATION DISTANCE

Since Γ_1 is a form of the complex signal correlation function it is possible to obtain the signal decorrelation lengths in the x and y directions directly from the exponential terms of Equation 86. These important signal parameters are

$$l_{ox} = l_0 \quad (92a)$$

$$l_{oy} = \frac{l_0}{\Delta} \quad (92a)$$

l_{ox} and l_{oy} are measures of the average distance between fades at the receiver location and depend on the path geometry. The quantity Δ is given by Equation 32 and gives the effect of the variation in the angle of propagation with respect to the magnetic field direction. Another useful measure of the signal decorrelation properties is the signal decorrelation time which is a measure of the inverse fading rate or fading bandwidth. The signal decorrelation time is given by the equations

$$t_{ox} = \frac{l_{ox}}{V_{xeff}} \quad (93a)$$

$$t_{oy} = \frac{l_{oy}}{V_{yeff}} \quad (93b)$$

where V_{xeff} and V_{yeff} are the velocity components of the line-of-sight at the receiver location. Although this velocity is a function of transmitter and receiver motion as well as irregularity motion, it is sufficient to consider the case where the transmitter and receiver are stationary and the phase-screen is in motion. Assume that the scattering layer consists of striations moving in unison at the velocity $V_x \hat{i} + V_y \hat{j}$ where \hat{i} and \hat{j} are unit vectors in the x and y directions, respectively. Consider only the y component of motion as shown for thin screen case in Figure 3. The projection of the striations at the receiver location due to a signal originating at $-z_t$ has velocity

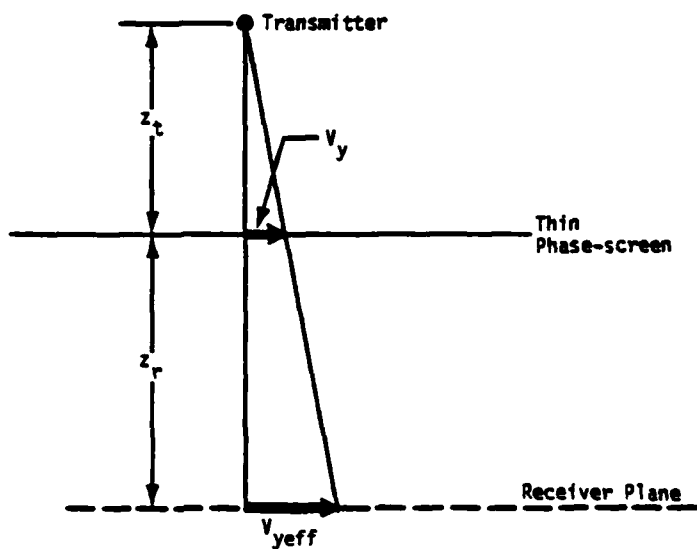


Figure 3. Thin phase-screen propagation geometry.

$$v_{y\text{eff}} = \frac{v_y (z_r + z_t)}{z_t} \quad (94)$$

Using this result for the y component of the velocity at the receiver, and a similar result for the x component of velocity, one obtains for the signal decorrelation time

$$t_{ox} = \left(\frac{A_0}{\sigma_\phi^2 A_2 v_x^2} \right)^{1/2} \quad (95a)$$

$$t_{oy} = \frac{1}{\Delta} \left(\frac{A_0}{\sigma_\phi^2 A_2 v_y^2} \right)^{1/2} \quad (95b)$$

Substituting the values of A_0 , A_2 and σ_ϕ for a Gaussian PSD one obtains as a final result

$$\begin{aligned}
 t_{0x} &= \frac{r_0}{\sigma_\phi V_x} \\
 &= \frac{r_0^{1/2}}{\pi^{1/4} (q\Delta L)^{1/2} \lambda r_e \sigma_{N_e} V_x} \quad (96a)
 \end{aligned}$$

$$\begin{aligned}
 t_{0y} &= \frac{r_0}{\Delta \sigma_\phi V_y} \\
 &= \frac{r_0^{1/2}}{\pi^{1/4} (q\Delta^3 L)^{1/2} \lambda r_e \sigma_{N_e} V_y} \quad (96b)
 \end{aligned}$$

where both forms are given for convenience.

At this point the solution for the two-position, two-frequency mutual coherence function is complete. The result for the thick scattering layer given by Equation 77 is simplified by taking the thin phase-screen limit. In this limit the result is given by Equation 86 in terms of the quantities σ_ϕ , Δ , λ_0 and ω' . These quantities are basic parameters that describe the propagation environment and geometry. The quantity σ_ϕ is the phase standard deviation and describes the strength of the scintillation. The decorrelation distance of the complex electric field is λ_0 in the x-direction and is λ_0/Δ in the y-direction. It will be seen that the parameter ω' is related to the coherence bandwidth which is a measure of the maximum bandwidth modulated signal that can propagate through the layer without multipath distortion.

In the following the effects of an aperture receiving antenna on the measured values of signal decorrelation distance and coherence bandwidth are determined.

SECTION 3

ANTENNA APERTURE EFFECTS ON RECEIVED SIGNAL

An antenna aperture acts to coherently collect the energy incident upon the antenna and to deliver it to the receiver. In the transmitting mode a directive antenna is designed to transmit energy only over a selected angular region. In the receiving mode this same directive antenna accepts energy only from a narrow range of angles. Thus, relative to an omnidirectional point antenna, a directive antenna will experience what is referred to as angular scattering loss when the signal at the aperture exhibits scintillation. This angular scattering loss arises from angle-of-arrival jitter present in the incident wavefront that may cause energy to arrive at the antenna propagating at angles greater than those accepted by the receiving aperture.

A different but equivalent way to view the effect of a receiving antenna aperture is as a coherent integrator of the signal arriving on the aperture face. If the antenna is pointing towards the source of an undisturbed plane wave, then the antenna output is maximum. If there are fluctuations in the signal phase across the aperture or the incident wavefront is tilted relative to the antenna boresight direction, the coherent integrator output is decreased.

As another aspect of the aperture averaging effect, an antenna can act to increase the measured decorrelation distance at the antenna output. This observed increase is caused by the averaging effect of the coherent integration that smooths the more rapid fluctuations.

Similarly the antenna acts to cut off signals that are incident at large angles from boresight. In severe scintillation this off-boresight energy propagates over longer paths than the more direct energy incident at boresight. For this reason a narrow beam antenna that does not accept off-axis contributions acts to reduce the observed time delay jitter of the output signal and thereby to increase the observed coherence bandwidth.

3.1 APERTURE ANTENNA FORMULATION

Consider the case of a spherical wave that originates from a transmitter located at $(0,0,-z_t)$ and propagates in free-space in the positive z direction where it is incident on a thin layer of irregularities located at $z=0$. After emerging from the irregularities, the wave again propagates in free-space to a receiving aperture antenna located in the plane $z=z_r$.

If the incident field in the plane of the antenna is $U(\bar{\rho}, z_r, \omega)$ then the complex voltage envelope at the antenna output may be expressed as (Price, Chesnut and Burns, 1972)

$$v(\bar{\rho}_0, z_r, \omega) = \int U(\bar{\rho}', z_r, \omega) A^*(\bar{\rho}' - \bar{\rho}_0) d^2\rho' \quad (97)$$

where

U = the solution to the parabolic wave equation at location $\bar{\rho}'$ in the receiver plane for a monochromatic signal frequency of ω .

$\bar{\rho}_0$ = the location of the center of the aperture antenna

A^* = the complex antenna weighting function

In this section all single and multiple integrations on infinite limits will be written using a single integral sign with no limits shown.

It is recognized that Equation 97 is a convolution so that

$$v(\bar{K}) = U(\bar{K}, z_r, \omega) A^*(\bar{K}) \quad (98)$$

where the Fourier transforms are given by

$$U(\bar{K}, z_r, \omega) = \frac{1}{4\pi^2} \int U(\bar{\rho}, z_r, \omega) \exp(-i\bar{K} \cdot \bar{\rho}) d^2\rho \quad (99)$$

$$A(\bar{K}) = \frac{1}{4\pi^2} \int A(\bar{\rho}) \exp(-i\bar{K} \cdot \bar{\rho}) d^2\rho \quad (100)$$

and the vector \bar{K} is

$$\bar{K} = k \sin\theta (\cos\phi \hat{i} + \sin\phi \hat{j}) \quad (101)$$

for the geometry shown in Figure 4.

The received voltage envelope at the antenna output may then be written as the inverse Fourier transform

$$v(\bar{\rho}_0, z_r, \omega) = 4\pi^2 \int U(\bar{K}, z_r, \omega) A^*(\bar{K}) \exp(i\bar{K} \cdot \bar{\rho}_0) d^2K \quad (102)$$

Since $A(\bar{K})$ represents the antenna voltage gain in the direction \bar{K} , it is possible to write the effect of changing the antenna pointing direction as

$$v(\bar{\rho}_0, z_r, \omega, \bar{K}_0) = 4\pi^2 \int U(\bar{K}, z_r, \omega) A^*(\bar{K} - \bar{K}_0) \exp(i\bar{K} \cdot \bar{\rho}_0) d^2K \quad (103)$$

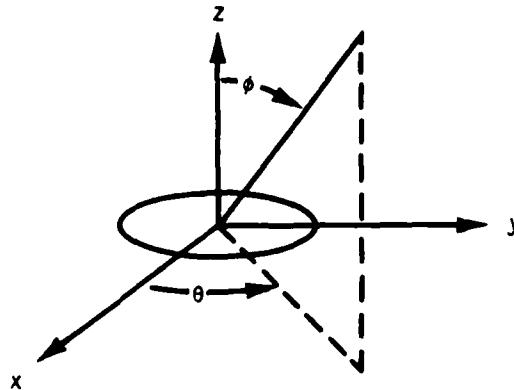


Figure 4. Receiving antenna aperture centered at origin of coordinate system.

where only the antenna voltage gain function has been affected by the new pointing direction. By replacing U and A by their Fourier transforms and performing the integrations, Equation 103 can be written in the form

$$v(\bar{\rho}_0, z_r, \omega, \bar{K}_0) = \exp(i\bar{K}_0 \cdot \bar{\rho}_0) \int U(\bar{\rho}', z_r, \omega) \times A^*(\bar{\rho}' - \bar{\rho}_0) \exp(-i\bar{\rho}' \cdot \bar{K}_0) d^2\rho' \quad (104)$$

Equation 104 gives the voltage output from an aperture antenna centered at $\bar{\rho}_0$ and pointed in the \bar{K}_0 direction. This result is applicable to the case of a transmitted monochromatic sinusoidal waveform.

Now if the transmitted waveform is a pulse waveform modulated on a carrier, the transmitted signal can be expressed as

$$s(\tau) = \text{Re} \{ m(\tau) \exp(i\omega_0 \tau) \} \quad (105)$$

where ω_0 is the carrier radian frequency and $m(\tau)$ is the modulation waveform. After passage through a layer of irregularities the received signal may be written (Knepp, 1982) in the absence of an antenna, as

$$r(\bar{\rho}, z_r, \tau) = \text{Re} \left\{ e(\bar{\rho}, z_r, \tau - \tau_d) \exp[i(\omega_0 \tau + \theta_0)] \right\} \quad (106)$$

where

$$e(\bar{\rho}, z_r, \tau) = \frac{1}{2\pi} \int_{-\infty}^{\infty} M(\omega) U(\bar{\rho}, z_r, \omega + \omega_0) \exp(i\omega\tau) d\omega \quad (107)$$

The quantity e is called the complex envelope of the received waveform. $M(\omega)$ is the Fourier transform of the transmitted modulation waveform and is given by

$$M(\omega) = \int_{-\infty}^{\infty} m(\tau) \exp(-i\omega\tau) d\tau \quad (108)$$

The quantities θ_0 and τ_d are the mean phase shift and time delay incurred after propagation through the ionization and are given as

$$\theta_0 = -\frac{\omega_0}{c} \int_{-z_t}^{z_r} (1 - \omega_p^2/\omega_0^2)^{1/2} dz' \quad (109)$$

$$\tau_d = \frac{1}{c} \int_{-z_t}^{z_r} (1 - \omega_p^2/\omega_0^2)^{-1/2} dz' \quad (110)$$

In order to obtain the effect of the antenna on the received time-domain waveform, the received complex envelope U in Equation 107 is replaced by its equivalent value v given by Equation 104. Thus the received time-domain signal at the antenna output may be written as

$$e(\bar{\rho}_0, z_r, \tau, \bar{K}_0) = \frac{1}{2\pi} \int M(\omega) U(\bar{\rho}', z_r, \omega + \omega_0) \times A^*(\bar{\rho}' - \bar{\rho}_0) \exp(-i\bar{\rho}' \cdot \bar{K}_0 + i\omega\tau) d^2\rho' d\omega \quad (111)$$

where the phase term $\exp(i\bar{K}_0 \cdot \bar{\rho}_0)$ has been omitted since it is constant. In the case that the receiving aperture is a point antenna, A^* is a delta function and the received complex envelope given by Equation 111 is identical to the result given by Equation 107.

The correlation function of the received power is given from Equation 111 as

$$\begin{aligned} \langle e(\bar{\rho}_1, \tau) e^*(\bar{\rho}_2, \tau) \rangle &= \frac{1}{4\pi^2} \int M(\omega') M^*(\omega'') \langle U(\bar{\rho}', \omega' + \omega_0) U^*(\bar{\rho}'', \omega'' + \omega_0) \rangle \\ &\times A^*(\bar{\rho}' - \bar{\rho}_1) A(\bar{\rho}'' - \bar{\rho}_2) \\ &\times \exp[-i(\bar{\rho}' - \bar{\rho}'') \cdot \bar{K}_0 + i(\omega' - \omega'')\tau] d\omega' d\omega'' d^2\rho' d^2\rho'' \end{aligned} \quad (112)$$

where the z_r dependence has been omitted and it is assumed that interest is focused on only the \bar{K}_0 pointing direction. Recognize that the term in the angle brackets is the two-position, two-frequency mutual coherence function, and is only a function of the difference in position and frequency, $\Gamma(\bar{\rho}' - \bar{\rho}'', \omega' - \omega'')$. With this in mind introduce the sum and difference transformations

$$\bar{\rho}_d = \bar{\rho}' - \bar{\rho}'' \quad (113)$$

$$\bar{\rho}_s = \frac{1}{2} (\bar{\rho}' + \bar{\rho}'')$$

$$\omega_d = \omega' - \omega'' \quad (114)$$

$$\omega_s = \frac{1}{2} (\omega' + \omega'')$$

to obtain for the correlation function of received power

$$\begin{aligned} \langle e(\bar{\rho}_1, \tau) e^*(\bar{\rho}_2, \tau) \rangle &= \frac{1}{4\pi^2} \int \Gamma(\bar{\rho}_d, \omega_d) M(\omega_s + \omega_d/2) M^*(\omega_s - \omega_d/2) \\ &\quad \times A^*(\bar{\rho}_s + \bar{\rho}_d/2 - \bar{\rho}_1) A(\bar{\rho}_s - \bar{\rho}_d/2 - \bar{\rho}_2) \\ &\quad \times \exp(-i\bar{\rho}_d \cdot \bar{K}_0 + i\omega_d \tau) d\omega_d d\omega_s d^2\rho_d d^2\rho_s \end{aligned} \quad (115)$$

In order to simplify this equation it is convenient to consider the case that the transmitted power is a delta function of delay. Since $M(\omega)$ is the Fourier transform of the transmitted complex envelope, the time-domain representation is given by

$$m(\tau) = \frac{1}{2\pi} \int M(\omega) \exp(i\omega\tau) d\omega \quad (116)$$

Thus the input power can be written as

$$P(t) = m(t)m^*(t) = \frac{1}{4\pi^2} \int M(\omega') M(\omega'') \exp[i(\omega' - \omega'')t] d\omega' d\omega'' \quad (117)$$

Now under the sum and difference transformations above the input power can be written as

$$I(t) = \frac{1}{4\pi^2} \int M(\omega_s + \omega_d/2) M^*(\omega_s - \omega_d/2) \exp(i\omega_d t) d\omega_d d\omega_s \quad (118)$$

Now if the input power is a delta function

$$I(t) = \delta(t) = \frac{1}{2\pi} \int \exp(i\omega_d t) d\omega_d \quad (119)$$

Comparison of Equations 118 and 119 yields for an input power delta function,

$$\frac{1}{2\pi} \int M(\omega_s + \omega_d/2) M^*(\omega_s - \omega_d/2) d\omega_s = 1 \quad (120)$$

Equation 120 above may be used to obtain the received power correlation function for an input power delta function

$$\begin{aligned} G(\bar{\rho}_1 - \bar{\rho}_2, \tau) &= \frac{1}{2\pi} \int \Gamma(\bar{\rho}_d, \omega_d) \\ &\quad \times A^*(\bar{\rho}_s + \bar{\rho}_d/2 - \bar{\rho}_1) A(\bar{\rho}_s - \bar{\rho}_d/2 - \bar{\rho}_2) \\ &\quad \times \exp(-i\bar{\rho}_d \cdot \bar{K}_0 + i\omega_d \tau) d\omega_d d^2\rho_d d^2\rho_s \end{aligned} \quad (121)$$

where the notation G is used for this important function. At this point introduce the Fourier transform of the antenna aperture distribution as given by the Fourier transform of Equation 100

$$A(\bar{\rho}) = \int A(\bar{K}) \exp(i\bar{K} \cdot \bar{\rho}) d^2k \quad (122)$$

Substitution of Equation 122 into Equation 121 gives

$$\begin{aligned}
G(\bar{\rho}_1 - \bar{\rho}_2, \tau) &= \frac{1}{2\pi} \int \Gamma(\bar{\rho}_d, \omega_d) A^*(\bar{K}') A(\bar{K}'') \\
&\times \exp[-i\bar{\rho}_s \cdot (\bar{K}' - \bar{K}'') - i \frac{\bar{\rho}_d}{2} \cdot (\bar{K}' + \bar{K}'') \\
&+ i\bar{K}' \cdot \bar{\rho}_1 - i\bar{K}'' \cdot \bar{\rho}_2 - i\bar{\rho}_d \cdot \bar{K}_0 + i\omega_d \tau] d\omega_d d^2 \rho_d d^2 \rho_s d^2 K' d^2 K''
\end{aligned} \tag{123}$$

The ρ_s integration yields the delta function $4\pi^2 \delta(\bar{K}' - \bar{K}'')$ and enables one to then easily perform the K'' integration. The result is then

$$\begin{aligned}
G(\bar{\rho}_1 - \bar{\rho}_2, \tau) &= 2\pi \int \Gamma(\bar{\rho}_d, \omega_d) |A(\bar{K})|^2 \\
&\times \exp [i\bar{K} \cdot (\bar{\rho}_1 - \bar{\rho}_2) - i(\bar{K} + \bar{K}_0) \cdot \bar{\rho}_d + i\omega_d \tau] d\omega_d d^2 \rho_d d^2 \bar{K}
\end{aligned} \tag{124}$$

To additionally simplify this expression introduce the generalized power spectrum (Wittwer, 1980; Knepp 1982) which is the Fourier transform of the mutual coherence function,

$$S(\bar{K}, \tau) = \frac{1}{8\pi^3} \int \Gamma(\bar{\rho}_d, \omega_d) \exp(-i\bar{K} \cdot \bar{\rho}_d + i\omega_d \tau) d\omega_d d^2 \rho_d \tag{125}$$

Utilization of the generalized power spectrum in Equation 124 yields for the power impulse response function at the aperture output

$$\begin{aligned}
G(\bar{\rho}_1 - \bar{\rho}_2, \tau) &= (2\pi)^4 \int S(\bar{K} + \bar{K}_0, \tau) |A(\bar{K})|^2 \\
&\times \exp [i\bar{K} \cdot (\bar{\rho}_1 - \bar{\rho}_2)] d^2 K
\end{aligned} \tag{126}$$

A simple change of variables yields the final result

$$\begin{aligned}
G(\bar{\rho}_1 - \bar{\rho}_2, \tau) &= (2\pi)^4 \int S(\bar{K}, \tau) |A(\bar{K} - \bar{K}_0)|^2 \\
&\times \exp [i(\bar{K} - \bar{K}_0) \cdot (\bar{\rho}_1 - \bar{\rho}_2)] d^2 K
\end{aligned} \tag{127}$$

Taking $\bar{\rho}_1 = \bar{\rho}_2$ gives the mean power at the antenna output due to a transmitted power delta function

$$G(0, \tau) = (2\pi)^4 \int S(\bar{K}, \tau) |A(\bar{K} - \bar{K}_0)|^2 d^2K \quad (128)$$

It is easy to verify that the above equation has the correct normalization. For a point receiving antenna $A(\bar{\rho}) = \delta(\bar{\rho})$ and therefore

$$A(\bar{K}) = \frac{1}{4\pi^2} \quad (129)$$

and the mean received power impulse response function becomes

$$G(0, \tau) = \int S(\bar{K}, \tau) d^2K \quad (130)$$

which is identical to previous results (Knepp, 1982) that were derived for the case of no antenna or equivalently, a point antenna.

Equation 128 can be written in another very useful form with the substitution

$$\hat{\Gamma}(\bar{K}, \omega_d) = \frac{1}{4\pi^2} \int \Gamma(\bar{\rho}_d, \omega_d) \exp(-i\bar{K} \cdot \bar{\rho}_d) d^2\rho_d \quad (131)$$

where $\hat{\Gamma}(\bar{K}, \omega_d)$ is the Fourier transform of the mutual coherence function. If $\hat{\Gamma}$ is used in Equation 124 one obtains

$$G(0, \tau) = (2\pi)^3 \int \hat{\Gamma}(\bar{K} + \bar{K}_0, \omega_d) |A(\bar{K})|^2 \exp(i\omega_d \tau) d\omega_d d^2K \quad (132)$$

or, changing variables,

$$G(0, \tau) = (2\pi)^3 \int \hat{\Gamma}(\bar{K}, \omega_d) |A(\bar{K} - \bar{K}_0)|^2 \exp(i\omega_d \tau) d\omega_d d^2K \quad (133)$$

It will be seen that Equation 133 is preferable for the evaluation of the effects of antennas on mean time delay and time delay jitter.

It is easy to compute $\hat{\Gamma}$ directly from Equation 131 using the thin screen approximation for the two-position, two-frequency mutual coherence function given by Equation 86. The result is

$$\begin{aligned} \hat{\Gamma}(K, \omega_d) = & \frac{\ell_0^2}{4\pi\Delta} \exp \left\{ -\frac{\sigma_\phi^2 \omega_d^2}{2\omega_0^2} \right\} \\ & \times \exp \left\{ -\frac{K_x^2 \ell_0^2}{4} \left(1+i \frac{\omega_d}{\omega'}\right) - \frac{K_y^2 \ell_0^2}{4\Delta^2} \left(1+i \frac{\omega_d}{\omega'/\Delta^2}\right) \right\} \end{aligned} \quad (134)$$

The generalized power spectrum may now be computed by using the expression just given for $\hat{\Gamma}$ and by applying the relationships of Equation 125 and 131 to obtain

$$\begin{aligned} S(K, \tau) = & \frac{\ell_0^2 \alpha \omega'}{2^{5/2} \pi^{3/2} \Delta} \exp \left\{ -\frac{K_x^2 \ell_0^2}{4} - \frac{K_y^2 \ell_0^2}{4\Delta^2} \right\} \\ & \times \exp \left\{ -\frac{\alpha^2}{2} \left[\omega' \tau - \frac{(K_x^2 + K_y^2) \ell_0^2}{4} \right]^2 \right\} \end{aligned} \quad (135)$$

where

$$\alpha = \frac{\omega_0}{\sigma_\phi \omega'} \quad (136)$$

For a Gaussian irregularity power spectrum, the parameter α may be calculated using the expression for ω' given by Equation 88 as

$$\alpha = \frac{\lambda z_r z_t \sigma_\phi}{\pi(z_t + z_r) r_0^2} \quad (137)$$

It is apparent that α is a measure of the severity of the scattering since it is directly proportional to the phase standard deviation.

3.2 APERTURE DISTRIBUTION FUNCTION

Let the antenna be modeled as a Gaussian beam with gain function

$$G_a(\theta) = G_0 \exp(-\theta^2/\theta_0^2) \quad (138)$$

where the beamwidth θ_0 is related to the effective aperture diameter D by

$$\theta_0^2 = \left(\frac{\lambda}{D}\right)^2 / (4 \ln 2) \quad (139)$$

where λ is the wavelength at the carrier frequency. With this choice of θ_0

$$G_a(\lambda/2D) = G_0/2 \quad (140)$$

so that this Gaussian aperture has approximately the same 3 dB beamwidth as a uniformly illuminated circular antenna.

The antenna gain pattern is the square of the transform of the aperture response function defined earlier. Thus

$$A(\bar{K}) = |G_a(\theta)|^{1/2} = G_0^{1/2} \exp(-\theta^2/2\theta_0^2) \quad (141)$$

Equation 122 may be used to find the aperture weighting function $A(\bar{\rho})$. Then since

$$\bar{K} \cdot \bar{\rho} = k \sin \theta (x \cos \phi + y \sin \phi) \quad (142)$$

$$d\bar{K} = k^2 \sin \theta \cos \theta \, d\theta \, d\phi \quad (143)$$

the substitutions

$$x = \rho \cos \phi'$$

$$y = \rho \sin \phi'$$

yield, after performing the azimuthal integration

$$A(\bar{\rho}) = 2\pi k^2 G_0^{1/2} \int_0^{\pi} J_0(k\rho \sin\theta) \exp(-\theta^2/2\theta_0^2) \sin\theta \cos\theta \, d\theta \quad (144)$$

For small θ_0 most of the contribution to this integral comes from small values of θ . Thus it is possible to replace the sine of the angle with the angle itself and to extend the upper limit to infinity (Ratcliffe, 1956). The resulting expression is available in standard integral tables (Gradshteyn and Ryzhik, 1965) with the result

$$A(\bar{\rho}) = 2\pi k^2 \theta_0^2 G_0^{1/2} \exp(-k^2 \rho^2 \theta_0^2 / 2) \quad (145)$$

Since, in the small angle approximation,

$$K^2 = k^2 \sin^2 \theta = k^2 \theta^2 \quad (146)$$

Equation 141 may be written as

$$A(\bar{K}) = G_0^{1/2} \exp(-K^2 / 2k^2 \theta_0^2) \quad (147)$$

It is easy to verify that Equations 145 and 147 are Fourier transform pairs.

3.3 ANGULAR SCATTERING LOSS

The scattering loss and the effect of the antenna on measurements of decorrelation distance may both be calculated simultaneously by evaluation of Equation 127. Here only the limit of strong scattering (large σ_ϕ) and large coherence bandwidth (large ω_{coh} or ω') is considered. In that case the parameter α given by Equation 136 is small and the generalized power spectrum reduces to the simplified form

$$\lim_{\alpha \rightarrow 0} \overline{S(K, \tau)} = \frac{\ell_0^2 \alpha \omega'}{2^{5/2} \pi^{3/2} \Delta} \exp \left\{ -\frac{K_x^2 \ell_0^2}{4} - \frac{K_y^2 \ell_0^2}{4 \Delta^2} \right\} \\ \times \exp \left\{ -\frac{1}{2} (\alpha \omega' \tau)^2 \right\} \quad (148)$$

The factor $\alpha \omega'$ is equal to the ratio ω_0 / σ_ϕ and does not reduce to zero in the limit of small α .

The correlation function of the received power can easily be evaluated for the case of a Gaussian antenna beam. Using Equations 147 and 148 in Equation 127 one obtains

$$G(\overline{\rho}_1 - \overline{\rho}_2, \tau) = \frac{(2\pi)^4 G_0 \alpha \omega' \exp \left\{ -\frac{1}{2} (\alpha \omega' \tau)^2 \right\}}{(2\pi)^{1/2} [(1 + 0.28 D^2 / \ell_0^2)(1 + 0.28 \Delta^2 D^2 / \ell_0^2)]^{1/2}} \\ \times \exp \left\{ \frac{-\zeta^2 / \ell_0^2}{1 + 0.28 D^2 / \ell_0^2} - \frac{\eta^2 / (\ell_0^2 / \Delta^2)}{1 + 0.28 \Delta^2 D^2 / \ell_0^2} \right\} \quad (149)$$

where it is assumed that the antenna boresight is in the z-direction and therefore $\overline{K}_0 = 0$. In Equation 149

$$\overline{\rho}_1 - \overline{\rho}_2 = (\zeta, \eta)$$

and the antenna beamwidth θ_0 is written in terms of λ/D as given by Equation 139. For an omnidirectional receiving antenna whose aperture diameter approaches zero, the gain G_0 goes to $1/(2\pi)^4$ and

$$\lim_{D \rightarrow 0} G(0, \tau) = \frac{\alpha \omega'}{(2\pi)^{1/2}} \exp \left\{ -\frac{1}{2} (\alpha \omega' \tau)^2 \right\} \quad (150)$$

which is identical to earlier results for the power impulse response function neglecting antenna aperture effects (Knepp, 1982).

The ratio of the correlation function of the received signal envelope (Equation 149) to the received power with no antenna (that is, with a wide-beamwidth point antenna) gives the aperture antenna effect as

$$\frac{G(\bar{\rho}_1 - \bar{\rho}_2, \tau)}{\lim_{D \rightarrow 0} G(0, \tau)} = \frac{1}{[(1+0.28D^2/\ell_0^2)(1+0.28\Delta^2D^2/\ell_0^2)]^{1/2}} \times \exp \left\{ -\frac{\zeta^2/\ell_0^2}{1+0.28D^2/\ell_0^2} - \frac{n^2/(\ell_0^2/\Delta^2)}{1+0.28\Delta^2D^2/\ell_0^2} \right\} \quad (151)$$

The angular scattering loss is given by the term in the square bracket

$$\text{loss} = [(1+0.28D^2/\ell_0^2)(1+0.28\Delta^2D^2/\ell_0^2)]^{1/2} \quad (152)$$

Equation 152 gives the angular scattering loss as a function of antenna diameter and various properties of the scattering medium and scattering geometry. In order to separate geometric effects from antenna effects note that the decorrelation distance (with no antenna) is given by Equation 90 repeated here

$$\ell_0^2 = \frac{(z_t + z_r)^2 r_0}{\sqrt{\pi} (\lambda r_e)^2 q \Delta L z_t^2 \sigma_{N_e}^2}$$

where the factor Δ gives the effect of varying the inclination angle. For propagation parallel to the magnetic field line $\psi=0$ and $\Delta=1$. Therefore define the new parameter ℓ_p as the decorrelation distance for parallel propagation as

$$\ell_p^2 = \Delta \ell_0^2 = \frac{(z_t + z_r)^2 r_0}{\sqrt{\pi} (\lambda r_e)^2 q L z_t^2 \sigma_{N_e}^2} \quad (153)$$

As can be seen λ_p is not a function of the propagation geometry. Now the angular scattering loss can be written in terms of λ_p as

$$\text{loss} = [(1+0.28\Delta D^2/\lambda_p^2)(1+0.28\Delta^3 D^2/\lambda_p^2)]^{1/2} \quad (154)$$

which explicitly gives the effect of variations in the antenna aperture size and of variations in the scattering geometry.

As seen from Equation 151 and the following, the effect of the antenna aperture is easily interpreted as a function of the ratio of the antenna diameter to the decorrelation distance of the field incident on the aperture. It is easily shown that these results may equivalently be interpreted in terms of the ratio of the rms scattering angle to the antenna beamwidth. From the Appendix and Equation 139 relating the antenna beamwidth and diameter one obtains

$$\frac{D}{\lambda_0} = \frac{\pi}{(2\ln 2)^{1/2}} \frac{\sigma_{\theta x}}{\theta_0} \quad (155)$$

$$\frac{\Delta D}{\lambda_0} = \frac{\pi}{(2\ln 2)^{1/2}} \frac{\sigma_{\theta y}}{\theta_0} \quad (156)$$

where $\sigma_{\theta x}$ and $\sigma_{\theta y}$ are the rms angle-of-arrival fluctuations measured along the x- and y-axes, respectively.

Thus since

$$\frac{0.28 D^2}{\lambda_0^2} = \frac{2 \sigma_{\theta x}^2}{\theta_0^2} \quad (157)$$

$$\frac{0.28 \Delta^2 D^2}{\ell_0^2} = \frac{2 \sigma_{\theta y}^2}{\theta_0^2} \quad (158)$$

it is apparent that antenna aperture effects become important only when the rms scattering angle approaches or exceeds the antenna beamwidth. This statement is true for all the effects considered here; the severity of the effect depends upon the particular measurement.

Figure 5 shows the scattering loss in decibels as a function of the field inclination angle for a value of the axial ratio q of 15. In all succeeding figures q is taken as 15 (Wittwer, 1979). The ratio of the antenna diameter to the decorrelation distance for parallel propagation D/ℓ_p is shown parametrically for the values 1, 3, 10, 30 and 100. Figure 6 is another plot of Equation 154 and shows the angular scattering loss as a function of the normalized antenna diameter D/ℓ_p for values of the inclination angle of 0° , 15° , 30° , 45° and 90° . It is seen in both figures that only when the antenna diameter is large with respect to the decorrelation distance is the angular scattering loss significant. Small inclination angles cause increased values of the phase standard deviation σ_ϕ and thus give increased angular scattering and increased scattering loss as shown. An increase in the inclination angle causes a decrease in σ_ϕ , an effective increase in the true decorrelation distance and therefore causes a decrease in the effect of angular scattering loss.

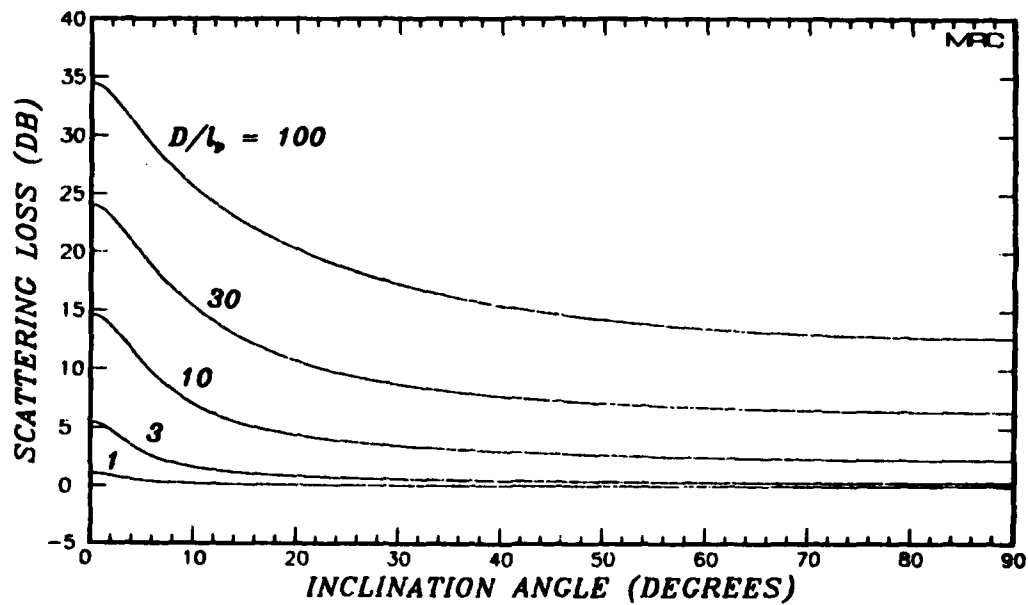


Figure 5. Angular scattering loss as a function of the magnetic field inclination angle.

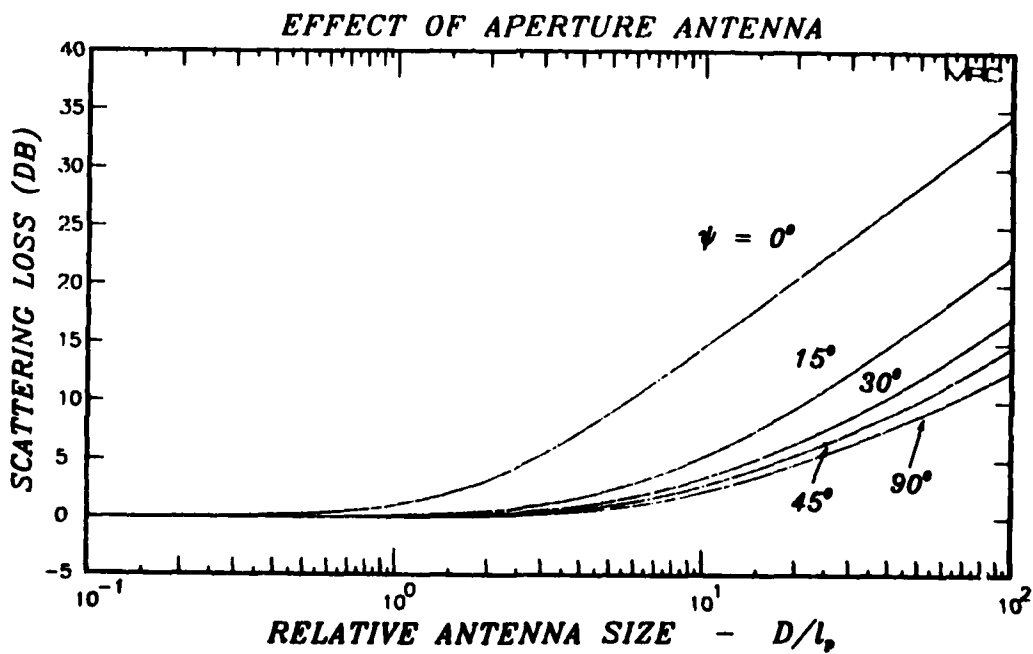


Figure 6. Angular scattering loss as a function of the aperture diameter.

3.4 SIGNAL DECORRELATION DISTANCE

The effect of the aperture on the measured correlation function is given by the two terms in the exponential of Equation 151 as

$$\ell_x = \ell_0 (1 + 0.28D^2/\ell_0^2)^{1/2} \quad (159)$$

$$\ell_y = (\ell_0/\Delta)(1 + 0.28\Delta^2 D^2/\ell_0^2)^{1/2} \quad (160)$$

where ℓ_x is the antenna measured decorrelation distance in the x-direction and ℓ_y is the same quantity measured in the y-direction. These quantities differ because of the geometry of propagation with respect to the magnetic field direction. For propagation parallel to the magnetic field line $\Delta=1$ and $\ell_x=\ell_y$. Similarly for isotropic irregularities $q=1$ and $\Delta=1$ and D is not a function of the field inclination angle so that $\ell_x=\ell_y$ again. With a point receiver, $D=0$, and the measured decorrelation distances are ℓ_0 and ℓ_0/Δ as given by Equations 92a and 92b as well as Equations 159 and 160.

The decorrelation distances in the x- and y-directions may be normalized by their values measured by an omnidirectional (point) antenna and plotted as

$$\frac{\ell_x}{\ell_0} = (1 + 0.28\Delta D^2/\ell_p^2)^{1/2} \quad (161)$$

$$\frac{\ell_y}{(\ell_0/\Delta)} = (1 + 0.28\Delta^3 D^2/\ell_p^2)^{1/2} \quad (162)$$

Figure 7 shows the relative decorrelation distance in the x-direction as a function of inclination angle for values of D/ℓ_p of 1, 3, 10, 30 and 100. The axial ratio q is taken as 15. Figure 8 shows the relative decorrelation distance in the x-direction as a function of the normalized

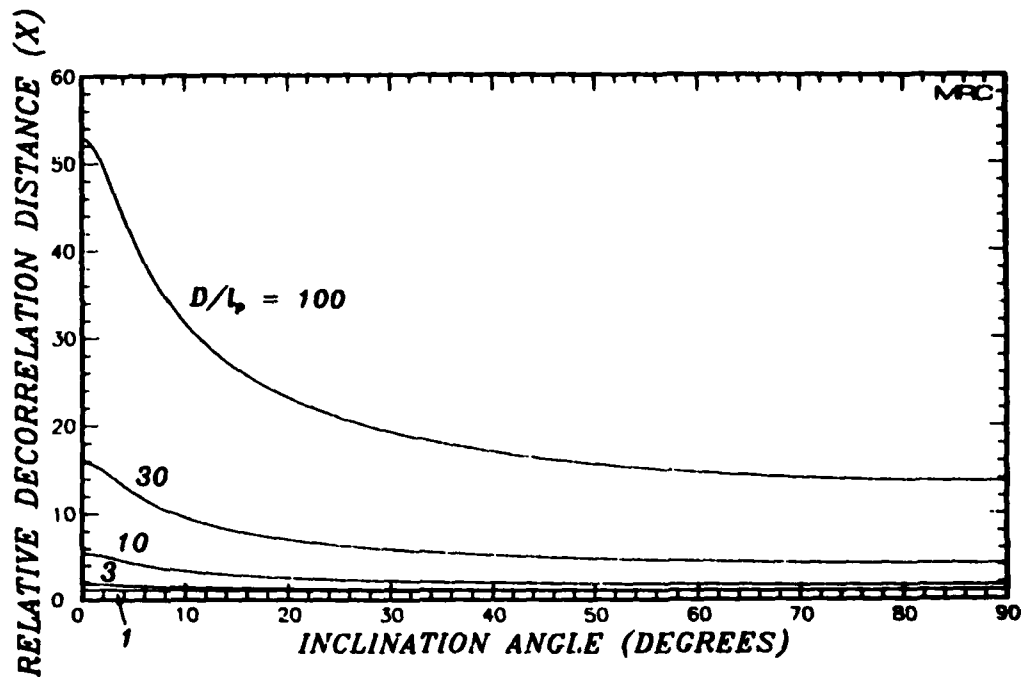


Figure 7. Effect of aperture and magnetic field direction on measured decorrelation distance in the x-direction.

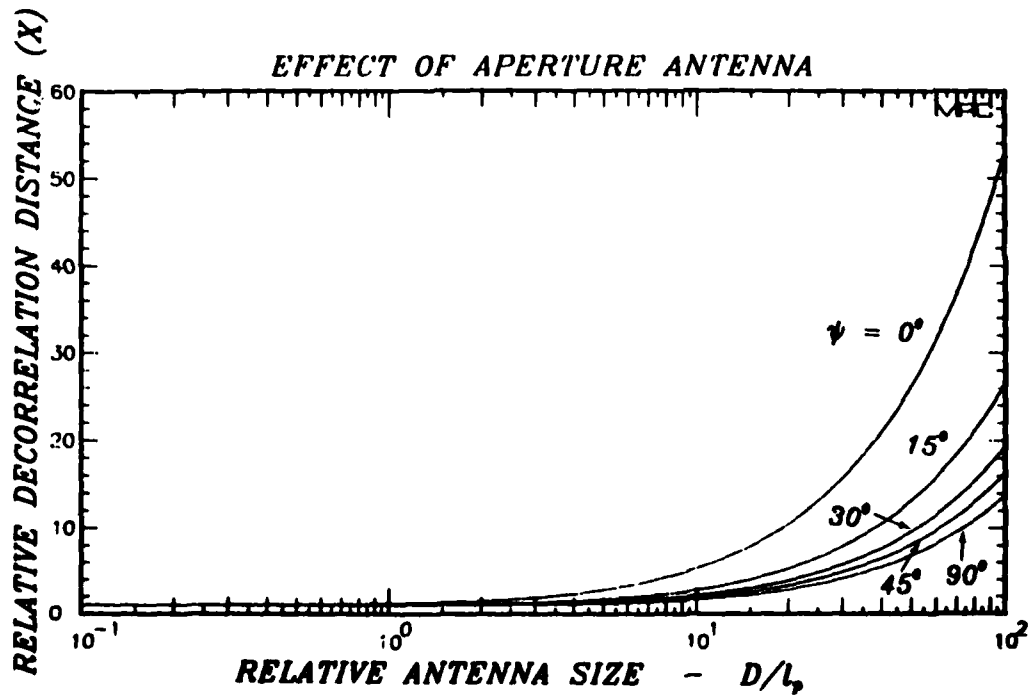


Figure 8. Effect of aperture and magnetic field direction on measured decorrelation distance in the x-direction.

antenna diameter for values of the inclination angle of 0°, 15°, 30°, 45° and 90°. Figure 8 shows that antennas with diameters less than the decorrelation distance do not affect measurements of angular scattering. From Figures 7 and 8 it is evident that very large antennas can greatly increase the measured decorrelation distance (relative to a point antenna) for sufficiently strong angular scattering at small inclination angles.

Figures 9 and 10 show the effect of an aperture antenna on measured values of the decorrelation distance in the y-direction. The format of these two figures is identical to the format of Figures 7 and 8. In the y-direction the effect of the antenna aperture is much smaller than in the x-direction for values of inclination angle greater than about 10°.

3.5 ANTENNA APERTURE EFFECT ON $\langle \tau \rangle$ and σ_τ

In the same manner than an aperture antenna with a finite beamwidth neglects or averages out energy incident at off-boresight angles to reduce the received power, it also acts to reduce the measured time delay and time delay jitter. This reduction occurs because the energy arriving from directions away from boresight typically travels over longer paths than the more direct signal. These longer paths require a longer propagation time and hence contribute to increased $\langle \tau \rangle$ and σ_τ values. If this energy is neglected by an aperture antenna, then the signal at the output will be characterized by smaller $\langle \tau \rangle$ and σ_τ than that measured by an omnidirectional (point) antenna.

Now define the mean time delay, $\langle \tau \rangle$, as

$$\langle \tau \rangle = \frac{\int G(0, \tau) \tau d\tau}{\int G(0, \tau) d\tau} \quad (163)$$

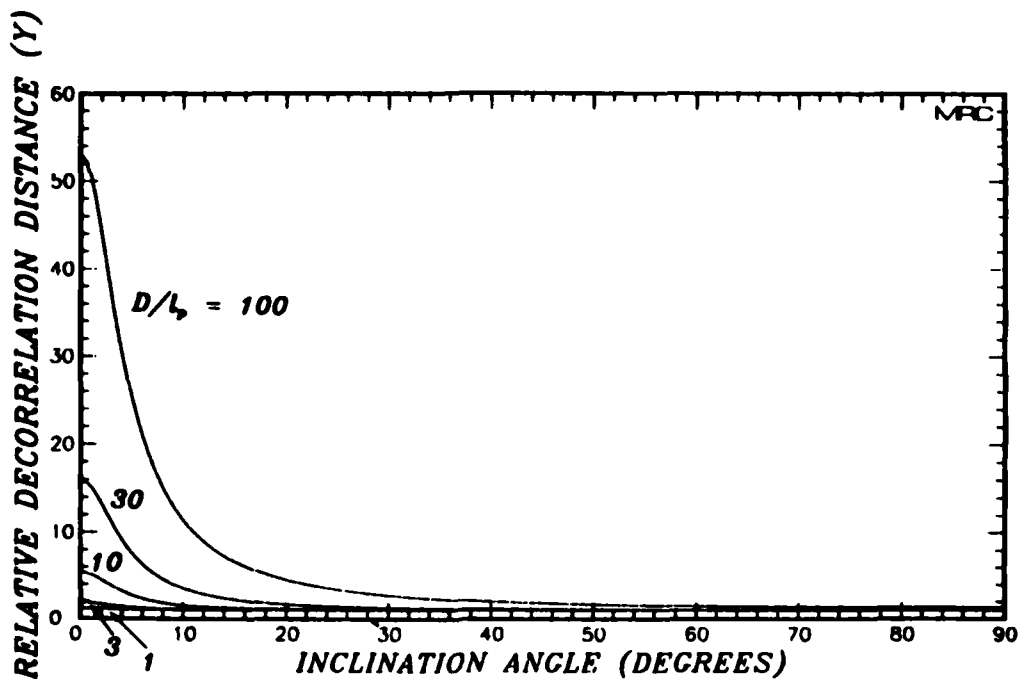


Figure 9. Effect of aperture and magnetic field direction on measurements of the decorrelation distance in the y-direction.

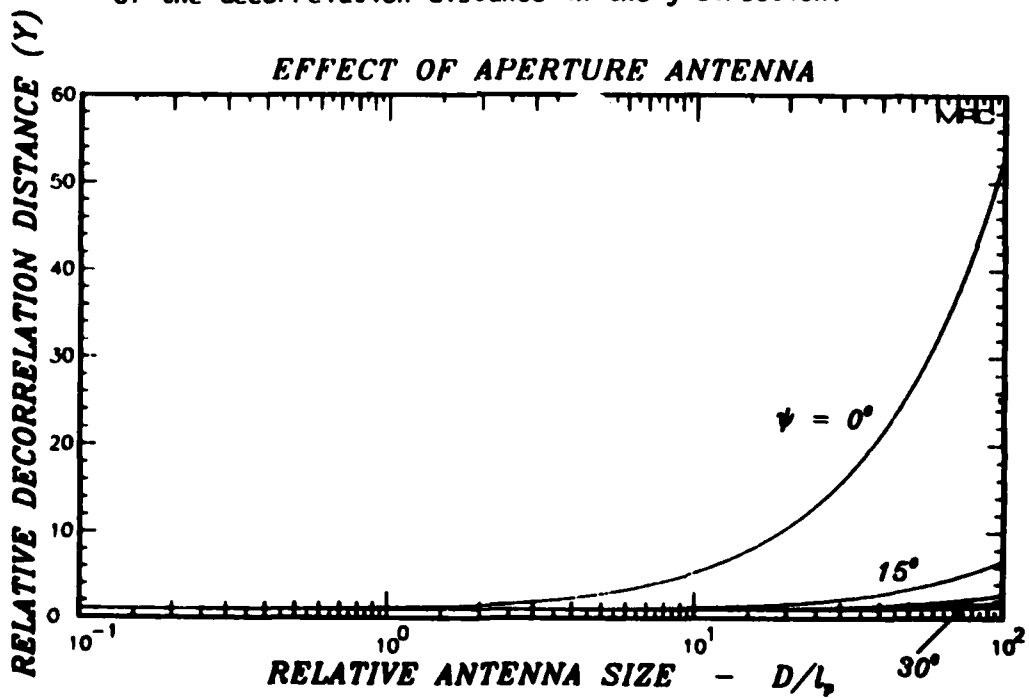


Figure 10. Effect of aperture and magnetic field direction on measurements of the decorrelation distance in the y-direction.

and define the time delay jitter σ_τ , by the second moment

$$\sigma_\tau^2 = \frac{\int G(0, \tau) \tau^2 d\tau}{\int G(0, \tau) d\tau} - \langle \tau \rangle^2 \quad (164)$$

where $G(0, \tau)$ is the response measured at the output of the receiving antenna due to an impulse of power originating from the transmitter. Now the alternative expression for $G(0, \tau)$ given by Equation 133 is the choice for the evaluation of the mean time delay and the time delay jitter. In this case the integrals with respect to τ give Dirac delta functions and derivatives of Dirac delta functions. That is

$$\int \hat{\Gamma}(\bar{K}, \omega_d) \exp(i\omega_d \tau) d\tau = 2\pi \hat{\Gamma}(\bar{K}, 0) \quad (165)$$

$$\int \hat{\Gamma}(\bar{K}, \omega_d) \exp(i\omega_d \tau) \tau d\tau = i2\pi \left. \frac{\partial \hat{\Gamma}(\bar{K}, \omega)}{\partial \omega_d} \right|_{\omega_d=0} \quad (166)$$

$$\int \hat{\Gamma}(\bar{K}, \omega_d) \exp(i\omega_d \tau) \tau^2 d\tau = -2\pi \left. \frac{\partial^2 \hat{\Gamma}(\bar{K}, \omega_d)}{\partial \omega_d^2} \right|_{\omega_d=0} \quad (167)$$

Utilizing Equations 133 and 165-167 in the expressions for the mean time delay and the time delay jitter leaves only integrals over \bar{K} . For the Gaussian antenna beam used previously these integrals are easily performed with the result that, in terms of the antenna diameter

$$\langle \tau \rangle = \frac{1}{2\omega'} \left\{ \frac{1}{1+0.28D^2/\lambda_0^2} + \frac{\Delta^2}{1+0.28\Delta^2 D^2/\lambda_0^2} \right\} \quad (168)$$

and

$$\sigma_\tau^2 = \frac{1}{\alpha^2 \omega'^2} + \frac{1}{2} \left\{ \frac{1}{(1+0.28D^2/\lambda_0^2)^2} + \frac{\Delta^4}{(1+0.28\Delta^2 D^2/\lambda_0^2)^2} \right\} \frac{1}{\omega'^2} \quad (169)$$

Since $\alpha\omega' = \sigma_\phi / \omega_0$ the first term in Equation 169 is proportional to the ratio of the phase standard deviation and the carrier radian frequency. This term is always small for GHz frequencies and may be neglected. The result for the time delay jitter is then

$$\sigma_\tau = \frac{1}{\sqrt{2} \omega'} \left\{ \frac{1}{(1+0.28D^2/\lambda_0^2)^2} + \frac{\Delta^4}{(1+0.28\Delta^2 D^2/\lambda_0^2)^2} \right\}^{1/2} \quad (170)$$

For point antennas with no directivity the mean time delay is given from Equation 170 as

$$\langle \tau(\text{point antenna}) \rangle = \frac{1}{2\omega'} (1+\Delta^2) \quad (171)$$

Thus the effect of the aperture antenna on the measured mean time delay is given by the ratio

$$\frac{\langle \tau(\text{with antenna}) \rangle}{\langle \tau(\text{point antenna}) \rangle} = \frac{(1+0.28\Delta^2 D^2/\lambda_0^2) + \Delta^2(1+0.28D^2/\lambda_0^2)}{(1+\Delta^2)(1+0.28D^2/\lambda_0^2)(1+0.28\Delta^2 D^2/\lambda_0^2)} \quad (172)$$

For a point antenna the time delay jitter is given by Equation 170 as

$$\sigma_\tau(\text{point antenna}) = \frac{1}{\sqrt{2} \omega'} (1+\Delta^4)^{1/2} \quad (173)$$

The effect of the receiving aperture is best measured by the ratio

$$\frac{\sigma_\tau(\text{with antenna})}{\sigma_\tau(\text{point antenna})} = \frac{\{(1+0.28\Delta^2 D^2/\lambda_0^2)^2 + \Delta^4(1+0.28D^2/\lambda_0^2)^2\}^{1/2}}{(1+\Delta^4)^{1/2}(1+0.28D^2/\lambda_0^2)(1+0.28\Delta^2 D^2/\lambda_0^2)} \quad (174)$$

3.5.1 Coherence Bandwidth

The coherence bandwidth is the inverse of the time delay jitter of the power impulse response function. From Equation 170

$$\omega_{\text{coh}} = \frac{\sqrt{2} \omega' (1+0.28D^2/k_0^2)(1+0.28\Delta^2D^2/k_0^2)}{\{(1+0.28\Delta^2D^2/k_0^2)^2 + \Delta^4(1+0.28D^2/k_0^2)^2\}^{1/2}} \quad (175)$$

With a point antenna, the measured coherence bandwidth becomes

$$\omega_{\text{coh}}(\text{point antenna}) = \frac{\sqrt{2} \omega'}{(1+\Delta^4)^{1/2}} \quad (176)$$

For isotropic irregularities, $q=1$ and therefore $\Delta=1$ so that $\omega_{\text{coh}}=\omega'$ as is given by Knepp (1982). For infinitely elongated irregularities q goes to infinity, Δ tends to zero and $\omega_{\text{coh}}=\sqrt{2} \omega'$ which also agrees with the previous results that were calculated without consideration of aperture averaging.

The effect of an aperture antenna on the measured coherence bandwidth is given by the ratio of the antenna measured coherence bandwidth to the coherence bandwidth with no antenna. This ratio is the reciprocal of Equation 174. Figures 11 and 12 show the effect of inclination angle and of aperture diameter on the measured coherence bandwidth. In both figures the ordinate is the relative coherence bandwidth given by the reciprocal of Equation 174. In Figure 11 the relative coherence bandwidth is shown as a function of the inclination angle between the direction of propagation and the magnetic field. Values of the ratio of the antenna diameter to the decorrelation distance for parallel propagation are shown parametrically. In Figure 12 the abscissa and the parametric quantity are exchanged. The two figures show that the aperture antenna has a strong effect in increasing the measured coherence bandwidth over

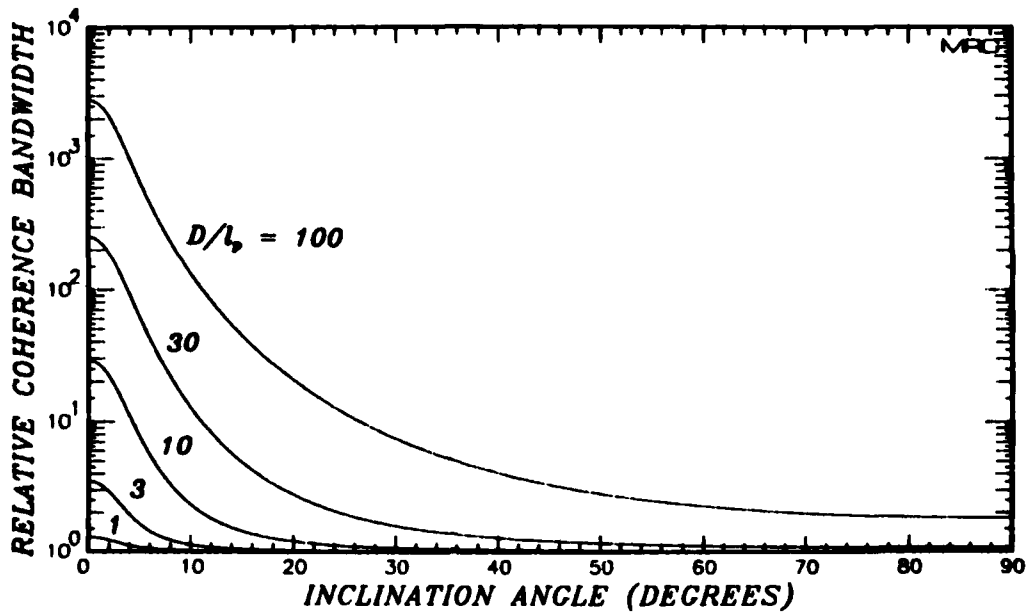


Figure 11. Effect of aperture and magnetic field direction on measurements of the coherence bandwidth.

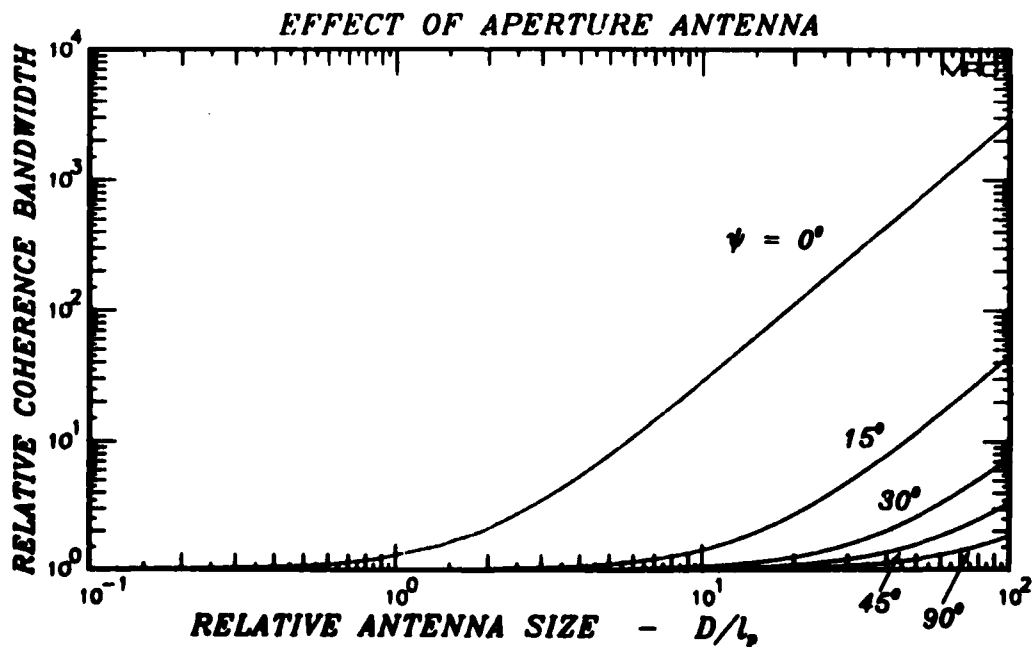


Figure 12. Effect of aperture and magnetic field direction on measurements of the coherence bandwidth.

the value given by an omnidirectional antenna especially for large apertures and propagation angles close to the magnetic field direction. This increased measurement of coherence bandwidth is caused by the action of the aperture to exclude or average out signals that are incident at large angles and hence have experienced greater delay than the directly incident signals. Equivalently, as discussed in conjunction with Equations 155-158, it is apparent that the aperture antenna significantly affects measurement of the coherence bandwidth whenever the rms angle-of-arrival fluctuation is greater than the antenna beamwidth.

Note that Figures 7-12 show the measured value of some signal parameter (measured with an aperture antenna) normalized by the value of that parameter measured by an omnidirectional antenna. That is, these figures present the effect of the aperture. Actual values of these parameters are easily calculated for any ionospheric condition and propagation geometry using the equations provided.

SECTION 4 SUMMARY

In this report results are presented that show the effect of non-isotropic irregularities on the two-position, two-frequency mutual coherence function. In addition the aperture averaging effect of a Gaussian antenna is determined for strong scattering conditions. It is shown that antennas that are larger in diameter than the decorrelation distance can experience significant angular scattering loss and cause increased measurements of decorrelation distance and coherence bandwidth relative to values measured with an omnidirectional antenna. Increases in measured decorrelation distance are caused by the averaging effect of the aperture that smooths the smaller scale signal fluctuations. Increased measurements of coherence bandwidth are caused by the action of the antenna to cut off signal contributions originating from off-boresight and which generally have experienced more delay than the direct signal incident at boresight.

Generally, the effects of aperture averaging begin to be significant for aperture sizes that are ten times the decorrelation distance. For still larger aperture dimensions, the aperture has a significant effect on the parameters that describe the received signal at the antenna output. However, this effect may be calculated using the formulas and curves provided herein.

REFERENCES

- Briggs, B. H., and I. A. Parkin, "On the Variation of Radio Star and Satellite Scintillations with Zenith Angle," J. Atmos. Terr. Phys., Vol. 25, pp. 339-365, 1963.
- Fante, R. L., "Electromagnetic Beam Propagation in Turbulent Media," Proc. IEEE, Vol. 63, No. 12, pp. 1669-1692, December 1975.
- Fante, R. L., "Some Physical Insights into Beam Propagation in Strong Turbulence," Radio Science, Vol. 15, No. 4, pp. 757-762, July-August 1980.
- Fante, R. L., "Two-position, Two-frequency Mutual-coherence Function in Turbulence," J. Opt. Soc. Am., Vol. 71, No. 12, pp. 1446-1451, December 1981.
- Gradshteyn, I. S., and I. M. Ryzhik, Tables of Integrals, Series and Products, Academic Press: New York, 1965.
- Knepp, D. L., Propagation of Wide Bandwidth Signals Through Strongly Turbulent Ionized Media, DNA-TR-81-78, MRC-R-671, Mission Research Corporation, March 1982.
- Papoulis, A., Probability, Random Variables, and Stochastic Processes, McGraw Hill: New York, 1965.
- Price, G. H., W. G. Chesnut, and A. Burns, Monopulse Radar Propagation Through Thick, Structured Ionization, Special Report 4, Contract DASA01-69-C-0126, SRI Project 8047, Stanford Research Institute, April 1972.
- Ratcliffe, J. A., "Some Aspects of Diffraction Theory and Their Application to the Ionosphere," Reports on Progress in Physics, Vol. 19, pp. 188-267, The Physical Society, London, 1956.
- Salpeter, E. E., "Interplanetary Scintillations. I. Theory," Astrophys. J., Vol. 147, pp. 433-448, 1967.
- Sreenivasiah, I., A. Ishimaru, and S. T. Hong, "Two-frequency Mutual Coherence Function and Pulse Propagation in a Random Medium: An Analytic Solution to the Plane Wave Case," Radio Science, Vol. 11, No. 10, pp. 775-758, October 1976.

Sreenivasiah, I., and A. Ishimaru, "Beam Wave Two-frequency Mutual-coherence Function and Pulse Propagation in Random Media: An Analytic Solution," Applied Optics, Vol. 18, No. 10, pp. 1613-1618, May 1979.

Tatarskii, V. I., The Effects of the Turbulent Atmosphere on Wave Propagation, translated by Israel Program for Scientific Translations, National Technical Information Service, U.S. Department of Commerce, 1971.

Wandzura, S. A., "Meaning of Quadratic Structure Functions," J. Opt. Soc. Am., Vol. 70, No. 6, pp. 745-747, June 1980.

Wittwer, L. A., Radio Wave Propagation in Structured Ionization for Satellite Applications, DNA 5304D, Defense Nuclear Agency, December 1979.

Wittwer, L. A., A Trans-Ionospheric Signal Specification for Satellite C³ Applications, DNA 5662D, Defense Nuclear Agency, December 1980.

Yeh, K. C., and C. H. Liu, "An Investigation of Temporal Moments of Stochastic Waves," Radio Science, Vol. 12, No. 5, pp. 671-680, September-October 1977.

APPENDIX
EVALUATION OF RMS ANGLE-OF-ARRIVAL FLUCTUATION

Consider a plane wave traveling in the negative z-direction and incident in the x-y plane at an angle θ from the z-axis. The electric field is given by

$$E(x,y) = E_0 \exp \{ ik(\sin\theta x + \cos\theta z) \} \quad (\text{A-1})$$

where the $\exp(i\omega t)$ time dependence is suppressed. The angle-of-arrival measured along the x-axis is computed as

$$\theta_x = \frac{1}{ikE_0} \frac{\partial E(x,z)}{\partial x} \quad (\text{A-2})$$

This computation gives $\sin \theta$ which in the small angle limit, is approximately θ .

In the case of interest here the incident field is given as the solution to the parabolic wave equation and the angle-of-arrival may be measured in both x- and y-directions as

$$\theta_x = \frac{1}{ikU_0} \frac{\partial U(\bar{\rho}, z, \omega)}{\partial x} \quad (\text{A-3})$$

$$\theta_y = \frac{1}{ikU_0} \frac{\partial U(\bar{\rho}, z, \omega)}{\partial y} \quad (\text{A-4})$$

where the measurement depends on the frequency. At a single frequency the rms values of θ_x and θ_y are related to the second derivatives of the two-position mutual coherence function (Papoulis, 1965, p. 317)

$$\sigma_{\theta_x}^2 = - \frac{1}{k^2} \frac{\partial^2 \Gamma(\zeta, \eta, \omega_d = 0)}{\partial \zeta^2} \quad (\text{A-5})$$

$$\sigma_{\theta_y}^2 = - \frac{1}{k^2} \frac{\partial^2 \Gamma(\zeta, \eta, \omega_d = 0)}{\partial \eta^2} \quad (\text{A-6})$$

From Equation 86 in the text one obtains for the rms angle-of-arrival fluctuations

$$\sigma_{\theta_x} = \frac{\sqrt{2}}{k \ell_0} \quad (\text{A-7})$$

$$\sigma_{\theta_y} = \frac{\sqrt{2}}{k(\ell_0/\Delta)} \quad (\text{A-8})$$

DISTRIBUTION LIST

DEPARTMENT OF DEFENSE

Assistant to the Secretary of Defense
Atomic Energy
ATTN: Executive Asst

Command & Control Tech Ctr
ATTN: C-312, R. Mason
ATTN: C-650, G. Jones
ATTN: C-650
3 cy ATTN: C-650, W. Heidig

Defense Communications Agency
ATTN: Code 230
ATTN: Code 205
ATTN: J300 for Yen-Sun Fu

Defense Communications Engr Ctr
ATTN: Code R410, R. Craighill
ATTN: Code R410, N. Jones
ATTN: Code R410
ATTN: Code R123

Defense Intelligence Agency
ATTN: Dir
ATTN: DB-4C, E. O'Farrell
ATTN: DB, A. Wise
ATTN: DT-1B
ATTN: DC-7B

Defense Nuclear Agency
ATTN: NAFD
ATTN: RAAE, P. Lunn
ATTN: STNA
ATTN: RAAE
ATTN: NATD
3 cy ATTN: RAAE
4 cy ATTN: TITL

Deputy Under Secretary of Defense
Comm, Cmd, Cont & Intell
ATTN: Dir of Intelligence Sys

Defense Tech Info Ctr
12 cy ATTN: DD

Field Command
Defense Nuclear Agency, Det 1
Lawrence Livermore Lab
ATTN: FC-1

Field Command
Defense Nuclear Agency
ATTN: FCTT, W. Summa
ATTN: FCTXE
ATTN: FCTT, G. Ganong
ATTN: FCPR

Interservice Nuclear Weapons School
ATTN: TTV

Joint Chiefs of Staff
ATTN: C3S
ATTN: C3S, Evaluation Ofc, HD00

DEPARTMENT OF DEFENSE (Continued)

Joint Strat Tgt Planning Staff
ATTN: JLA, Threat Applications Div
ATTN: JLTW-2

National Security Agency
ATTN: W-32, O. Bartlett
ATTN: B-3, F. Leonard

Under Secretary of Defense for Rsch & Engrg
ATTN: Strategic & Space Sys, (OS)
ATTN: Strat & Theater Nuc Forces, B. Stephan

WWMCCS System Engrg Org
ATTN: J. Hoff

DEPARTMENT OF THE ARMY

Assistant Chief of Staff for Automation & Comm
ATTN: DAMO-C4, P. Kenny

Atmospheric Sciences Lab
ATTN: DELAS-EO, F. Niles

BMD Advanced Technology Ctr
ATTN: ATC-R, D. Russ
ATTN: ATC-T, M. Capps
ATTN: ATC-O, W. Davies
ATTN: ATC-R, W. Dickinson

BMD Systems Cmd
ATTN: BMDSC-HLE, R. Webb
2 cy ATTN: BMDSC-HW

Deputy Chief of Staff for Ops & Plans
ATTN: DAMO-RQC, C2 Div

Harry Diamond Labs
ATTN: Chief Div 20000
ATTN: DELHD-NW-R, R. Williams, 22000

US Army Chemical School
ATTN: ATZN-CM-CS

US Army Comm-Elec Engrg Instal Agency
ATTN: CCC-CED-CCO, W. Neuendorf
ATTN: CCC-EMEO-PED, G. Lane

US Army Communications Cmd
ATTN: CC-OPS-WR, H. Wilson
ATTN: CC-OPS-W

US Army Communications R&D Cmd
ATTN: DRDCO-COM-RY, W. Kesselman

US Army Foreign Science & Tech Ctr
ATTN: DRXST-SD

US Army Materiel Dev & Readiness Cmd
ATTN: DRCLDC, J. Bender

US Army Nuclear & Chem Agency
ATTN: Library

DEPARTMENT OF THE ARMY (Continued)

US Army Satellite Comm Agency
ATTN: Doc Con

US Army TRADOC Sys Analysis Actvy
ATTN: ATAA-PL
ATTN: ATAA-TDC
ATTN: ATAA-TCC, F. Payan, Jr

US Army White Sands Missile Range
ATTN: STEWS-TN-N, K. Cummings

USA Missile Command
ATTN: DRSMI-YSO, J. Gamble

DEPARTMENT OF THE NAVY

Joint Cruise Missiles Project Ofc
ATTN: JCMG-707

Naval Air Systems Cmd
ATTN: PMA 271

Naval Electronic Systems Cmd
ATTN: PME 106-4, S. Kearney
ATTN: PME 117-20
ATTN: Code 3101, T. Hughes
ATTN: PME 106-13, T. Griffin
ATTN: PME 117-2013, G. Burnhart
ATTN: Code 501A
ATTN: PME 117-211, B. Kruger

Naval Intelligence Support Ctr
ATTN: NISC-50

Naval Ocean Systems Ctr
ATTN: Code 532
ATTN: Code 5323, J. Ferguson
ATTN: Code 5322, M. Paulson

Naval Research Lab
ATTN: Code 4780
ATTN: Code 4780, S. Ossakow
ATTN: Code 4187
ATTN: Code 7500, B. Wald
ATTN: Code 4700
ATTN: Code 4720, J. Davis
ATTN: Code 7950, J. Goodman
ATTN: Code 6700

Naval Space Surveillance System
ATTN: J. Burton

Naval Surface Weapons Ctr
ATTN: Code F31

Naval Telecommunications Cmd
ATTN: Code 341

Office of the Deputy Chief of Naval Ops
ATTN: NOP 981N
ATTN: NOP 654, Strat Eval & Anal Br
ATTN: NOP 941D

Office of Naval Rsch
ATTN: Code 414, G. Joiner
ATTN: Code 412, W. Condell

DEPARTMENT OF THE NAVY (Continued)

Strategic Systems Project Office
ATTN: NSP-2141
ATTN: NSP-43
ATTN: NSP-2722

Theater Nuclear Warfare Prj Office
ATTN: PM-23, D. Smith

DEPARTMENT OF THE AIR FORCE

Air Force Geophysics Lab
ATTN: OPR, H. Gardiner
ATTN: OPR-1
ATTN: LKB, K. Champion
ATTN: CA, A. Stair
ATTN: PHY, J. Buchau
ATTN: R. Babcock
ATTN: R. O'Neil

Air Force Tech Applications Ctr
ATTN: TN

Air Force Weapons Lab
ATTN: SUL
ATTN: NTYC
ATTN: NTN

Air Force Wright Aeronautical Lab/AAAD
ATTN: W. Hunt
ATTN: A. Johnson

Air Logistics Cmd
ATTN: OO-ALC/MM

Air University Library
ATTN: AUL-LSE

Assistant Chief of Staff
Studies & Analyses
ATTN: AF/SASC, W. Kraus
ATTN: AF/SASC, C. Rightmeyer

Ballistic Missile Office/DAA
ATTN: ENSN
ATTN: SYC, D. Kwan
ATTN: ENSN, W. Wilson

Deputy Chief of Staff
Rsch, Dev & Acq
ATTN: AFRDP
ATTN: AFRDS, Space Sys & C3 Dir

Deputy Chief of Staff
Plans & Operations
ATTN: AFXOKCD
ATTN: AFXOKS
ATTN: AFXOKT

Headquarters
Electronic Systems Div
ATTN: ESD/SCTE, J. Clark
ATTN: OCT-4, J. Deas
ATTN: SCS-2, G. Vinkels
ATTN: SCS-1E

DEPARTMENT OF THE AIR FORCE (Continued)

Foreign Technology Div
ATTN: TQTD, B. Ballard
ATTN: NIIS, Library

Rome Air Development Ctr
ATTN: OCS, V. Coyne
ATTN: TSLD

Rome Air Development Ctr
ATTN: EEP, J. Rasmussen

Headquarters
Space Command
ATTN: DC, T. Long

Space Div
ATTN: YGJB, W. Mercer
ATTN: YKM, E. Norton
ATTN: YKM, W. Alexander

Strategic Air Command
ATTN: NRT
ATTN: DCXT, T. Jorgensen
ATTN: XPFS
ATTN: DCS
ATTN: ADWAT, R. Wittler

DEPARTMENT OF ENERGY

Department of Energy
ATTN: DP-233

OTHER GOVERNMENT AGENCIES

Central Intelligence Agency
ATTN: OSWR/NED
ATTN: OSWR/SSD for K. Feuerpfel

Department of Commerce
National Bureau of Standards
ATTN: Sec Ofc for R. Moore

Department of Commerce
National Oceanic & Atmospheric Admin
ATTN: R. Grubb

National Telecommunications Sciences
ATTN: L. Berry
ATTN: A. Jean
ATTN: W. Utlaut

Department of State
Office of International Security Policy
ATTN: PM/STM

NATO

NATO School, SHAPE
ATTN: US Documents Officer

DEPARTMENT OF ENERGY CONTRACTORS

EG&G, Inc
ATTN: J. Colvin
ATTN: D. Wright

University of California
Lawrence Livermore National Lab
ATTN: L-389, R. Ott
ATTN: L-31, R. Hager
ATTN: Tech Info Dept, Library

Los Alamos National Lab
ATTN: MS 670, J. Hopkins
ATTN: P. Keaton
ATTN: MS 664, J. Zinn
ATTN: T. Kunkle, ESS-5
ATTN: R. Jeffries
ATTN: D. Simons
ATTN: J. Wolcott

Sandia National Labs
ATTN: B. Murphey
ATTN: T. Cook

Sandia National Labs
ATTN: D. Thornbrough
ATTN: Tech Library, 3141
ATTN: D. Dahlgren
ATTN: Space Project Div
ATTN: Org 4231, T. Wright
ATTN: Org 1250, W. Brown

DEPARTMENT OF DEFENSE CONTRACTORS

Aerospace Corp
ATTN: V. Josephson
ATTN: R. Slaughter
ATTN: T. Salmi
ATTN: I. Garfunkel
ATTN: K. Cho
ATTN: J. Straus
ATTN: D. Olsen

Analytical Systems Engrg Corp
ATTN: Radio Sciences

Analytical Systems Engrg Corp
ATTN: Security

BDM Corp
ATTN: T. Neighbors
ATTN: L. Jacobs

Berkeley Rsch Associates, Inc
ATTN: C. Prettie
ATTN: J. Workman
ATTN: S. Brecht

Boeing Aerospace Co
ATTN: MS/87-63, D. Clauson

DEPARTMENT OF DEFENSE CONTRACTORS (Continued)

Boeing Co
ATTN: G. Hall
ATTN: S. Tashird

BR Communications
ATTN: J. McLaughlin

University of California at San Diego
ATTN: H. Booker

Charles Stark Draper Lab, Inc
ATTN: D. Cox
ATTN: A. Tetewski
ATTN: J. Gilmore

Computer Sciences Corp
ATTN: F. Eisenbarth

Comsat Labs
ATTN: G. Hyde
ATTN: D. Fang

Cornell University
ATTN: D. Farley, Jr
ATTN: M. Kelly

E-Systems, Inc
ATTN: R. Berezdivin

Electrospace Systems, Inc
ATTN: H. Logston
ATTN: P. Phillips

EOS Technologies, Inc
ATTN: B. Gabbard

General Electric Co
ATTN: A. Steinmayer
ATTN: C. Zierdt

General Electric Co
ATTN: G. Millman

General Rsch Corp
ATTN: B. Bennett

GEO Centers, Inc
ATTN: E. Marram

GTE Communications Products Corp
ATTN: R. Steinhoff

GTE Communications Products Corp
ATTN: J. Concordia
ATTN: I. Kohlberg

Harris Corp
ATTN: E. Knick

Honeywell, Inc
ATTN: G. Terry, Avionics Dept
ATTN: A. Kearns, MS924-3

Horizons Technology, Inc
ATTN: R. Kruger

DEPARTMENT OF DEFENSE CONTRACTORS (Continued)

HSS, Inc
ATTN: D. Hansen

IBM Corp
ATTN: H. Ulander

Institute for Defense Analyses
ATTN: J. Aein
ATTN: E. Bauer
ATTN: F. Wolfhard
ATTN: H. Gates

International Tel Telegraph Corp
ATTN: Technical Library

International Tel & Telegraph Corp
ATTN: G. Wetmore

JAYCOR
ATTN: J. Sperling

Johns Hopkins University
ATTN: T. Evans
ATTN: K. Potocki
ATTN: J. Newland
ATTN: P. Komiske
ATTN: J. Phillips

Kaman Tempo
ATTN: B. Gambill
ATTN: K. Schwartz
ATTN: DAISAC
ATTN: J. Devore
ATTN: W. McNamara

Kaman Tempo
ATTN: DASIAC

Litton Systems, Inc
ATTN: B. Zimmer

Lockheed Missiles & Space Co, Inc
ATTN: J. Kumer
ATTN: R. Sears

Lockheed Missiles & Space Co, Inc
ATTN: Dept 60-12
2 cy ATTN: D. Churchill, Dept 62-A1

M.I.T. Lincoln Lab
ATTN: D. Towle

MA/COM Linkabit Inc
ATTN: A. Viterbi
ATTN: H. Van Trees
ATTN: I. Jacobs

Magnavox Govt & Indus Electronics Co
ATTN: G. White

McDonnell Douglas Corp
ATTN: Tech Library Svcs
ATTN: W. Olson
ATTN: R. Halprin

DEPARTMENT OF DEFENSE CONTRACTORS (Continued)

Meteor Communications Corp
ATTN: R. Leader

Mission Rsch Corp
ATTN: C. Lauer
ATTN: Tech Library
ATTN: F. Fajen
ATTN: R. Kilb
ATTN: S. Gutsche
ATTN: R. Bigoni
ATTN: R. Bogusch
ATTN: F. Guigliano
ATTN: G. McCartor
ATTN: R. Hendrick
4 cy ATTN: D. Knepp
5 cy ATTN: Doc Con

Mitre Corp
ATTN: MS J104, M. Dresp
ATTN: A. Kymmel
ATTN: G. Harding
ATTN: C. Callahan

Mitre Corp
ATTN: W. Hall
ATTN: J. Wheeler
ATTN: M. Horrocks
ATTN: W. Foster

Pacific-Sierra Rsch Corp
ATTN: E. Field, Jr
ATTN: F. Thomas
ATTN: H. Brode, Chairman SAGE

Pennsylvania State University
ATTN: Ionospheric Research Lab

Photometrics, Inc
ATTN: I. Kofsky

Physical Dynamics, Inc
ATTN: E. Fremouw

Physical Rsch, Inc
ATTN: R. Deliberis
ATTN: T. Stephens

R&D Associates
ATTN: R. Turco
ATTN: W. Karzas
ATTN: H. Ory
ATTN: C. Greifinger
ATTN: P. Haas
ATTN: M. Gantsweg
ATTN: F. Gilmore
ATTN: W. Wright

R&D Associates
ATTN: B. Yoon

Rand Corp
ATTN: B. Bennett

DEPARTMENT OF DEFENSE CONTRACTORS (Continued)

Rand Corp
ATTN: E. Bedrozian
ATTN: C. Crain
ATTN: P. Davis

Riverside Rsch Institute
ATTN: V. Trapani

Rockwell International Corp
ATTN: R. Buckner

Rockwell International Corp
ATTN: S. Quilici

Science Applications, Inc
ATTN: L. Linson
ATTN: D. Hamlin
ATTN: C. Smith
ATTN: E. Straker

Science Applications, Inc
ATTN: J. Cockayne

Science Applications, Inc
ATTN: M. Cross

SRI International
ATTN: R. Tsunoda
ATTN: J. Vickrey
ATTN: W. Chesnut
ATTN: R. Leadabrand
ATTN: R. Livingston
ATTN: D. McDaniels
ATTN: M. Baron
ATTN: G. Price
ATTN: D. Neilson
ATTN: A. Burns
ATTN: W. Jaye
ATTN: J. Petrickes
ATTN: C. Rino
ATTN: V. Gonzales
ATTN: G. Smith

Stewart Radiance Lab
ATTN: J. Ulwick

Technology International Corp
ATTN: W. Boquist

Toyon Rsch Corp
ATTN: J. Ise
ATTN: J. Garbarino

Tri-Com, Inc
ATTN: D. Murray

TRW Electronics & Defense Sector
ATTN: R. Plebuch
ATTN: G. Kirchner

DEPARTMENT OF DEFENSE CONTRACTORS (Continued)

Utah State University
Attention Sec Con Ofc for
ATTN: K. Baker, Dir Atmos & Space Sci
ATTN: L. Jensen, Elec Eng Dept
ATTN: D. Burt
ATTN: A. Steed

DEPARTMENT OF DEFENSE CONTRACTORS (Continued)

VisiDyne, Inc
ATTN: C. Humphrey
ATTN: O. Shepard
ATTN: W. Reidy
ATTN: J. Carpenter

D
FI